

BURSTS OF EXTENSIVE AIR SHOWERS: CHAOS VS. STOCHASTICITY

Yu. A. Fomin, G. V. Kulikov, M. Yu. Zotov*

Ultrahigh Energy Particles Laboratory
D. V. Skobeltsyn Institute of Nuclear Physics
M. V. Lomonosov Moscow State University, Moscow 119992, Russia

Abstract

Bursts of the count rate of extensive air showers (EAS) lead to the appearance of clusters in time series that represent EAS arrival times. We apply methods of nonlinear time series analysis to twenty EAS cluster events found in the data set obtained with the EAS-1000 prototype array. In particular, we use the Grassberger–Procaccia algorithm to compute the correlation dimension of the time series in the vicinity of the clusters. We find that four cluster events produce signs of deterministic chaos in the corresponding time series. By applying a number of supplementary methods we assess that the nature of the observed behaviour of the correlation dimension is likely to be deterministic. We compare our conclusions with the results of similar investigations performed by the EAS-TOP and LAAS groups.

1. Introduction

We have already studied the distribution of arrival times of extensive air showers (EAS) registered with the EAS-1000 prototype array both by methods of classical statistics [1, 2] and by methods of cluster analysis [3, 4]. In particular, we presented twenty EAS cluster events—groups of consecutive showers that were registered in time intervals much shorter than expected ones and thus present bursts of the EAS count rate, see [3, 4]. This phenomenon has put forward at least two questions: one on the astrophysical nature of the process, another on its statistical properties. Namely, while the vast majority of sufficiently long samples satisfy the hypothesis for an exponential distribution of time delays between EAS arrival times [1, 2], the χ^2 -test performed for samples taken in the vicinity of some of the EAS clusters made us reject this hypothesis. Thus we decided to apply methods of nonlinear time series analysis to samples that contain EAS clusters in order to clarify dynamical reasons of this situation.

Recall that the data set under consideration represents 203 days of regular operation of the array in the period from August 30, 1997 till February 1, 1999. The total EAS number in the data set equals 1 668 489. The mean interval between consecutive EAS arrival times is equal to 10.5 sec. The discreteness in the moments of EAS registration is approximately 0.055 sec (one tic of the PC clock).

In [5], we have already discussed briefly the results of nonlinear analysis of one of the EAS clusters. Here we go into details and give the results of a similar analysis of all clusters presented in [3] and [4].

2. Preliminary Facts

In what follows, we study a scalar time series of the form x_1, x_2, \dots, x_n , where $x_i = t_i - t_{i-1}$, t_i is the moment of registration of the i th EAS, $i = 1, \dots, n$, and $t_0 = 0$ corresponds to midnight. For the purposes of our investigation, it is convenient to use time intervals x_i given in seconds.

Our approach to the analysis of the time series is based on the ideas and results presented in [6, 7, 8] (see, e.g., [9] for a comprehensive review). The main tool to analyse the dynamics of the time series under consideration is the Grassberger–Procaccia method [10] with the modification suggested by Theiler [11]. Namely, given a sample (x_1, x_2, \dots, x_N) extracted from the time series we construct delay vectors

$$\mathbf{x}_i = (x_i, x_{i+\tau}, x_{i+2\tau}, \dots, x_{i+(m-1)\tau}),$$

* fomin, kulikov, zotov@eas.sinp.msu.ru

where τ is an arbitrary but fixed time increment and m is an embedding dimension. Then we compute the number $K(\rho)$ of vectors with mutual distance less or equal than ρ and such that delay vectors \mathbf{x}_i are shifted by at least W indices:

$$K(\rho) = \sum_{i=1}^{M-W} \sum_{j=i+W}^M \Theta(\rho - \|\mathbf{x}_i - \mathbf{x}_j\|), \quad (1)$$

where Θ is the Heaviside step function, $M = N - (m-1)\tau$, and $W \geq 1$ is the cut-off parameter (the Theiler window). Finally, we plot $\log K(\rho)$ versus $\log \rho$. For small ρ , the slope of this plot is an estimate of the correlation dimension D_2 :

$$D_2(\rho) = \frac{d \log C_2(\rho)}{d \log \rho},$$

where C_2 is the correlation sum:

$$C_2(\rho) = \frac{2K(\rho)}{(M-W)(M-W+1)}.$$

(Obviously, one may use K instead of C_2 in the expression for the correlation dimension.) A plateau observed in the $D_2(\rho)$ plot for small ρ or, equivalently, a so called scaling region in the $\log K$ vs. $\log \rho$ plot are regarded as signs of chaotic dynamics in the corresponding time series. A value of D_2 at the plateau is taken as an estimate of the correlation dimension of the attractor underlying the data. This quantity also gives a (lower) estimate for the number of degrees of freedom in the process under consideration.

To compute K , we normally divide each unit interval in $\lg \rho$ into 50 subintervals of equal length. We have found that though this number of subintervals seems to be small, it adequately reflects the qualitative structure of D_2 while a much bigger number of subintervals (≥ 200) leads to considerable fluctuations in D_2 ; these fluctuations hide the structure of D_2 , especially for m large enough. A smaller number of intervals gives too rough structure of D_2 . The derivative is calculated via a standard three-points algorithm. No smoothing or fitting procedures are used.

Notice that Eq. (1) contains four free parameters: N , τ , W , and m . At the preliminary stage of the investigation, we “scanned” the experimental data set having split it into adjacent samples with $N = 128, 256, 512, \text{ and } 1024$. At this step, we used $\tau = 1$, $W = 1$, and odd values of m in the range from 5 to 13. The value of N was chosen to be a power of 2 because this allows one to use fast algorithms of calculating the Fourier transform that is the main part of traditional Fourier analysis. After we have found a number of samples that demonstrated some kind of plateau in the plot of $D_2(\rho)$, we studied the corresponding data with different N in the above range and different values of τ in the range 1–10. (Evidently, in our case τ may take only integer values.) For N large enough, we have performed calculations for m up to 25. In any case, m and τ were chosen such that the number of delay vectors was greater than 100. Finally, to avoid autocorrelation in the time series, we employed $W = 1 \dots 20$.

To compute mutual distances between delay vectors [see Eq. (1)], we tried several norms: the maximum norm L_∞ : $\|\mathbf{z}\|_\infty = \sup_{1 \leq i \leq m} |z_i|$, the taxicab norm L_1 , and the Euclidian norm L_2 :

$$\|\mathbf{z}\|_1 = \sum_{i=1}^m |z_i|, \quad \|\mathbf{z}\|_2 = \sqrt{\sum_{i=1}^m |z_i|^2},$$

and the “dimension scaled” norms L_{1C} and L_{2C} [12, 13]:

$$\|\mathbf{z}\|_{1C} = \frac{1}{m} \|\mathbf{z}\|_1, \quad \|\mathbf{z}\|_{2C} = \frac{1}{\sqrt{m}} \|\mathbf{z}\|_2.$$

Since the process of calculating D_2 is very time consuming, we have used only one of these norms, namely the maximum norm, to scan the complete data set. Four other norms were tested at different samples both with and without a plateau in the $D_2(\rho)$ plot obtained with L_∞ .

There is a number of tools that can help to verify the results of calculating the correlation dimension D_2 . In particular, we used the Theiler–Takens “maximum likelihood” estimator of the correlation dimension [14, 15]:

$$t_{\text{TT}}(\rho) = C_2(\rho) \left[\int_0^\rho \frac{C_2(\rho')}{\rho'} d\rho' \right]^{-1}. \quad (2)$$

Another problem is to make an assessment about the nature of the dynamics in the case when a plateau in a plot of $D_2(\rho)$ is observed. The main difficulty is to figure out whether one witnesses chaotic dynamics in a deterministic process or a special class of stochastic processes [16, 17]. One of the main tools to solve this problem is the method of surrogate data [18, 19], see also [20] and references therein. Among other tools one can find the quantity

$$t_{\text{BDS}}(m, \rho) = \frac{C_2(m, \rho)}{C_2(1, \rho)^m} \quad (3)$$

suggested in [21] and in the above form—in [22]. As it was shown in [21], for a sequence of independent random numbers, $C_2(m, \rho) = C_2(1, \rho)^m$ holds, where m is the embedding dimension. Besides this, we used a function suggested in [23]:

$$\varphi_0(\rho) = \frac{D_2(m_2, \rho) - D_2(m_1, \rho)}{m_2 - m_1}, \quad (4)$$

where m_1 and m_2 are different embedding dimensions. For independent random data, $\varphi_0(\rho) \neq 0$ and $\varphi_0 \rightarrow 1$ as $\rho \rightarrow 0$. We also employed the “normalized slope” introduced in [13]:

$$\varphi(m, \rho) = \frac{1}{m} D_2(m, \rho). \quad (5)$$

If $\varphi(m, \rho)$ does not converge to 0 in a wide range of ρ as m grows but to some value ≥ 0.1 , then most probably data should be treated by statistical techniques [13].

Recall that before applying nonlinear techniques to the analysis of a time series, it is strongly suggested to check whether the time series is really nonlinear. Among other tools, one can try a measure for time-reversibility, which is considered to be a good indicator for nonlinearity [24]. For the data sorted in time order,

$$\gamma = \frac{1}{(\sigma^2)^{\frac{3}{2}}(N-1)} \sum_{i=2}^N \left(\frac{x_i - x_{i-1}}{t_i - t_{i-1}} \right)^3 \quad (6)$$

is calculated, which is just the mean of the slopes, taken to the third power (here σ^2 is the variance of the sample). For a time series generated by a linear process, and for the surrogate data, one expects $\gamma \approx 0$. In contrast, time series with nonlinearities can be asymmetrical in time and may yield values of $\gamma \neq 0$. To check, whether γ significantly deviates from zero for the studied sample, one should generate a sufficient number of surrogate data. To pay regard to deviations in both directions ($\gamma > 0$ and $\gamma < 0$), a two sided test has to be performed [18].

Finally, a few words are in order about stationarity of the time series under consideration. As is well known, a fundamental assumption underlying almost all existing linear and nonlinear techniques of time series analysis is that the time series is stationary, see, e.g., [25]. As we have already mentioned earlier [2, 4, 26], the count rate of EAS depends on the value of the atmospheric pressure. For the data obtained with the EAS-1000 prototype array, this dependence can be approximately expressed by a simple formula

$$\ln N = -\beta P + \text{const},$$

where N is the number of EAS registered in a time unit, P is the atmospheric pressure, mm Hg, and $\beta \approx 10^{-2}$ is the barometric coefficient. This effect makes the time series non-stationary. To provide stationarity (at large time scales) we adjusted time delays between consecutive showers to the atmospheric pressure $P^* = 742$ mm Hg which is close to the average pressure for the whole analyzed data set. This adjustment was made by the following formula:

$$x_i = x_i^0 \exp[\beta(P^* - P_i)],$$

where x_i^0 is the experimental time delay, and P_i is the atmospheric pressure at the i th delay. The barometric coefficient was chosen to be $\beta = 1.08 \cdot 10^{-2}$, exactly as in our previous paper [4]. Due to the adjustment, the mean and the variance of the time series at large time scales were approximately constant.

Remark. In fact, since we shall discuss only comparatively short samples, the above adjustment to P^* is not important for the present results because atmospheric pressure does not change significantly during

periods of time covered by the samples. We perform the adjustment in order to guarantee stationarity of the whole time series.

To compute the correlation sum C_2 effectively, we have worked out an algorithm based on preliminary sorting of mutual distances between delay vectors. Though quite simple, the algorithm occurred to be up to 10 times faster than a straightforward computation of C_2 . To perform calculations, we employed GNU Octave [27] running in Mandrake Linux.

3. The Main Results

As is well known, one needs sufficiently long samples to perform a successful time series analysis. On the other hand, the bursts of the EAS count rate have comparatively short time range. Thus we did not in fact expect to find signs of chaotic dynamics in the vicinity of EAS clusters. Surprisingly, we have found some.

Having “scanned” the available data set, we found that, as a rule, no scaling region is observed in $\log C_2$ vs. $\log \rho$ plots. This is quite natural since arrival times of extensive air showers represent a simple stochastic process such that for sufficiently long samples, the number of EAS registered in a time unit obeys the Poisson distribution in a wide range of time delays, see, e.g., [2]. Still, we have come across a number of samples with a plateau in the $D_2(\rho)$ plot in the vicinity of four EAS clusters, namely those registered on May 14, November 11, and December 28, 1998 and on January 8, 1999. Let us begin our discussion with the two longest events.

3.1. November 11, 1998

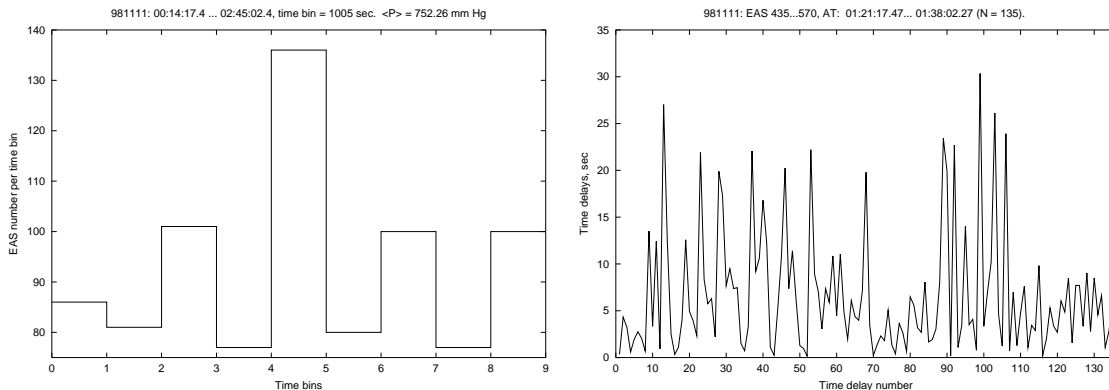


Figure 1: The count rate at a time interval that contains the cluster registered on November 11, 1998 (left); the cluster is presented by the central bin. Time delays (s) between EAS that constitute the cluster (right).

The cluster event observed on November 11, 1998 consists of 136 EAS registered within the period from 01:21:17.47 to 01:38:02.27 (Moscow local time) with the atmospheric pressure $P = 752.3$ mm Hg, see Fig. 1. Within the data set obtained on November 11, 1998 the showers that form the cluster event have numbers 435–570. The event is made up of three clusters, which begin at consecutive arrival times (i.e., the first cluster begins at the shower #435, the second one begins at the shower #436, etc.) and end up simultaneously at the shower #570. In our opinion, the appearance of three clusters does not reflect any process of astrophysical nature but is caused by the technique of their selection (see [4] for the details). Thus we treat the event as a single (outer) cluster. The real duration of this cluster equals 1004.8 s while the adjusted duration equals 898.8 s; the probability of the appearance of such a cluster is of the order of $2 \cdot 10^{-7}$. The maximum count rate within the cluster is observed in the period from 01:30:37.98 to 01:31:40.21 when 20 showers #503–522 have arrived.

Let us take a look at a number of samples in the vicinity of the cluster in order to see how the sum K and the correlation dimension D_2 change when the cluster appears. Recall that it is suggested for the Fourier analysis to have $x(1) \approx x(N)$. To satisfy this demand, we omit the last shower of the cluster and consider a sample that consists of 134 instead of 135 delays. Obviously, this does not influence K and D_2 significantly.

First, let us study a number of samples whose length is comparable with the length of the cluster. Fig. 2 presents plots of $D_2(\rho)$ (the left column) and $\lg K(\rho)$ (the right column) computed for $\tau = 1$, $W = 1$, and $m = 1 \dots 12$ for four samples in the vicinity of the cluster. The top row shows D_2 and $\lg K$ for a sample that begins approximately 41 min and ends 15 min before the cluster (EAS #225–365). Notice that even the upper curves of D_2 ($m \geq 10$) have sufficient statistics ($K > 100$) for $\lg \rho > 1.05$. No clear plateau is observed, though it seems that a kind of plateau tries to form at $\lg \rho \in (0.9, 1.0)$, but the number of close delay vectors is not sufficient at this range of ρ . Next comes a sample with the cluster (EAS #435–569). One can see an interval $\lg \rho \approx 0.94 \dots 1.12$ at which the correlation dimension saturates for $m \geq 7$ and fluctuates around $D_2 \approx 1.8 \pm 0.3$. Thus we conclude that the sample with the cluster demonstrates signs of chaotic dynamics with the (fractal) dimension of an attractor approximately equal to 1.8. For this interval in ρ , $\lg K \geq 2.5$ thus providing sufficient statistics. The third pair of plots presents D_2 and $\lg K$ for a sample that consists of the same number of time delays as the previous one, but begins approximately in the middle of the cluster (EAS #504–638). Notice an interesting behaviour of D_2 as m grows. First, there is a kind of plateau at $D_2 \approx 1.4$ for $\lg \rho \approx 0.96 \dots 1.6$ made up of curves obtained for $m = 4, 5, 6$. As m grows further, the plateau becomes longer and goes down to $D_2 \approx 0.8$. For this pair of plots, $m = 1 \dots 15$. At the interval where the plateau is observed, $\lg K > 2.2$ thus giving a sufficient number of delay vectors. Finally, the bottom pair of plots shows D_2 and $\lg K$ for a sample that begins in 15 min after the cluster (EAS #642–780). Clearly, no plateau is observed for this sample. In this sense, this plot is typical for our data set.

As one can see from the just discussed plots, the cluster drastically changes the behaviour of the correlation dimension. Let us notice that for both samples with a plateau the demand $m > 2D_2 + 1$ is satisfied if we assume that D_2 is given by the level of the corresponding plateau (see, e.g., [28]).

Now consider Fig. 3. As one can see from the top pair of plots, the Theiler–Takens estimator (2) does not have a plateau for the cluster, though there is an interval where the curves almost coincide for $m \geq 9$. Conversely, a clear plateau is observed for the second sample. We point out that its level is higher than the level of the plateau at the $D_2(\rho)$ plot and it is shifted slightly.

To assess whether the samples with the plateaus in the $D_2(\rho)$ plot present a special case of a stochastic process or chaotic behaviour in a deterministically driven system, let us study these samples in more details. As is clearly seen in Fig. 3, for higher m and both samples, $t_{\text{BDS}} \neq 1$ at the intervals where the plateaus are observed. The higher m is, the bigger deviation from zero is. Notice that while deviation from 1 is comparatively small for the cluster, it is very pronounced for the second sample. According to [21, 22], this gives an argument in favour of the conjecture that these two samples, especially the second one, do not represent a sequence of independent random numbers. As one can see from two other pairs of plots, this conjecture is also supported by the behaviour of the functions φ_0 and φ (φ_0 is computed for $m_2 - m_1 = 1$). All these quantities suggest that while the first sample (the cluster) does not exclude the possibility that it is extracted from a stochastic process, the second one is more likely to demonstrate deterministic chaos.

As we have mentioned above, one of the quantities that may be useful for the analysis of time series is the measure of time-reversibility γ , see Eq. (6). For the cluster, $\gamma = 0.74$ (we use $t_i - t_{i-1} = 1$). For the sample with EAS #504–638, $\gamma = -0.33$. To compare, $\gamma = -0.72$ for the sample before the cluster and $\gamma = -0.16$ for the sample after the cluster. It is interesting to note that $\gamma < 0$ for all these samples except for the cluster.

To estimate whether γ significantly deviates from zero and to clarify the situation with the samples that show a plateau in the $D_2(\rho)$ plot, we used the method of surrogate data. For each sample with a plateau, we generated 99 “shuffled” surrogates obtained by a random permutation of time intervals x_i in a given sample. This number of surrogates corresponds to a 98% level of significance (L.S.) of the statistical test [24]. The surrogates gave $\gamma \in (-1.38, 1.28)$ and $\gamma \in (-1.58, 1.38)$ for the cluster and the next sample respectively. Therefore, the null hypothesis for time-reversibility of the original samples cannot be rejected. Thus, this test does not detect nonlinearity in the samples under consideration. The same is true for the other two samples shown in Fig. 2.

On the other hand, if we analyse the behaviour of the correlation dimension D_2 for “shuffled” surrogates, then we find out that the plateaus disappear, and thus we conclude that the order of time delays that form these samples is important. To the contrary to the above test, this implies that both samples with a plateau represent a chaotic and thus nonlinear process.

To get a deeper insight into the nature of the samples in the vicinity of the cluster, we performed

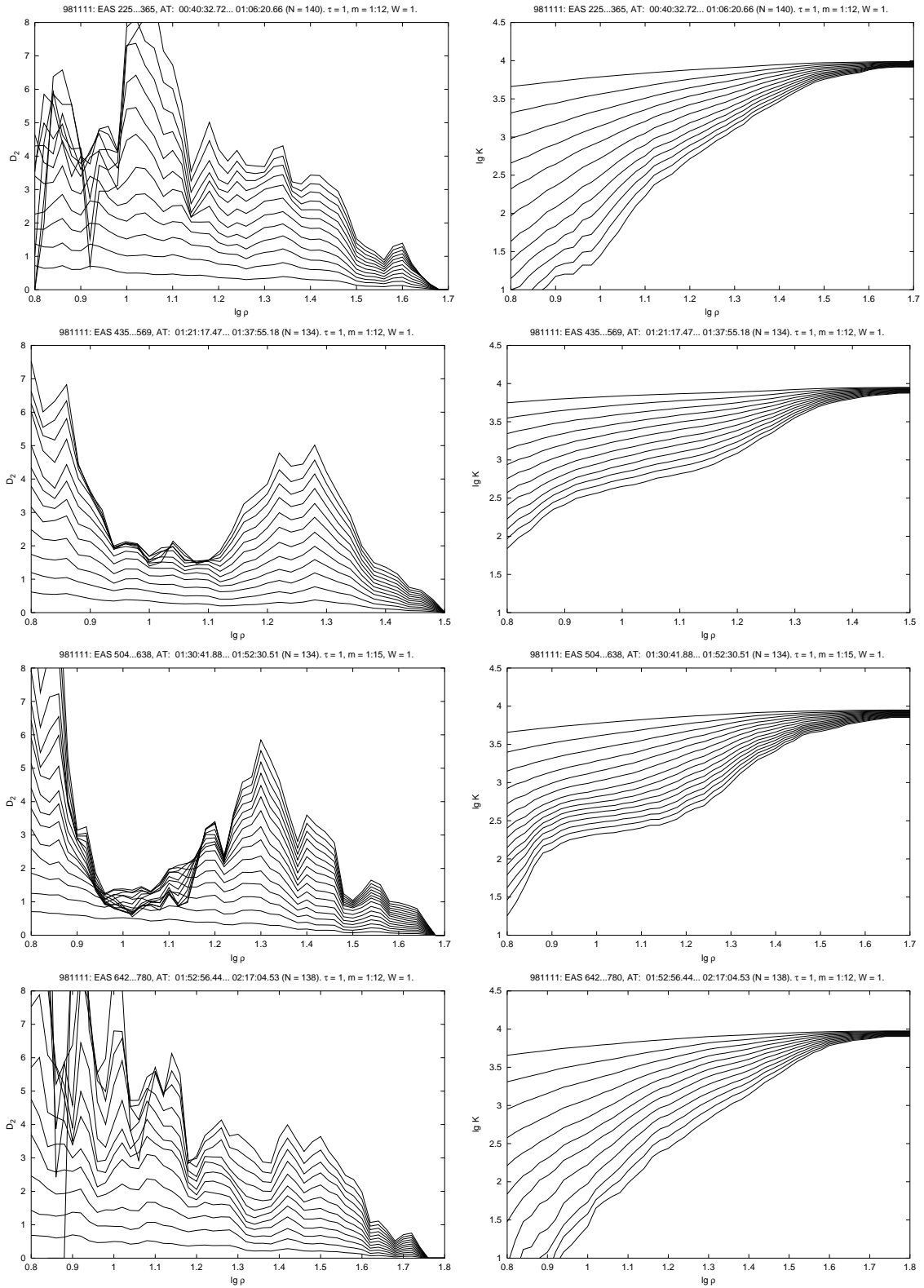


Figure 2: The correlation dimension $D_2(\rho)$ (the left column) and $\lg K(\rho)$ (the right column) for a number of samples in the vicinity of the cluster. From top to bottom: a sample before the cluster, a sample with the cluster (without the last delay), a sample with the second half of the cluster, and a sample after the cluster.

the χ^2 -test to verify the hypothesis that time delays between consecutive arrival times have an exponential distribution. We used different time bins in the range from 1 to 10 s with a step equal to 0.5 s providing that each bin taken into account contains more than 10 events. An acceptance or rejection of the χ^2 -test for this hypothesis strongly depends on the way of grouping time delays into bins. We have found that for the sample with the cluster, this hypothesis should be rejected with at least 90% L.S. On the other hand, for the sample made of EAS #504–638 one may accept the same hypothesis if 109 time delays that do not exceed 15 s are grouped into 5-second bins.

We have also made a number of exponentially distributed surrogates for this sample. They did not show a plateau in the $D_2(\rho)$ plot.

We have found that $\tau = 1$ is the only value for which a plateau for the sample with EAS #435–569 is observed. On the other hand, the value of W is not so important. As W grows, the plateau slightly deforms, but does not disappear. For the sample made of EAS #504–638, one can observe a plateau also for $\tau = 2$ and $m \leq 10$. For larger m , huge fluctuation of D_2 occur since the value of K is comparatively small for this range of $\lg \rho$. The value of W does not influence the behaviour of D_2 considerably.

A choice of the norm is crucial for the sample that contains the cluster. Namely, this sample does not have a plateau in the plot of the correlation dimension if other than L_∞ norm is used. A remarkable feature of the sample that consists of EAS #504–638 is that the choice of the norm is not so important. Namely, a plateau can be observed not only for the maximum norm, but also for the L_{1C} and L_{2C} norms.

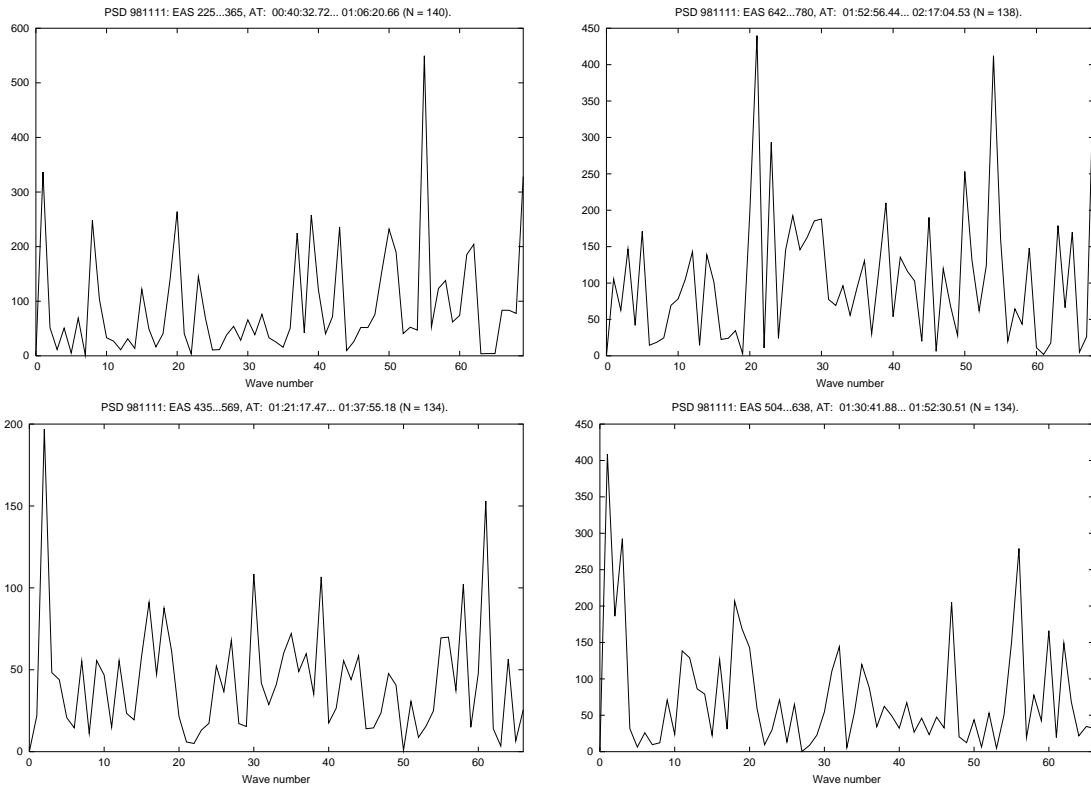


Figure 4: The power spectrum density for the samples made of EAS #225–365, 642–780 (the top row), and EAS #435–569 and 504–638 (the bottom row).

Besides nonlinear techniques, we have also used a classical approach based on the Fourier transform. Fig. 4 shows the power spectrum density for the four samples discussed above. One can see that the spectra do not differ considerably from a broadband one, though for each spectrum one can notice peaks that are much higher than the other ones. It is worth mentioning that for both samples with a plateau the highest peaks are located at the left end of the spectrum.

The choice of the sample with EAS #504–638 is more or less arbitrary. We have selected it to demonstrate the following tendency observed for samples with $N \sim 130$ –140. If a sample begins before the cluster

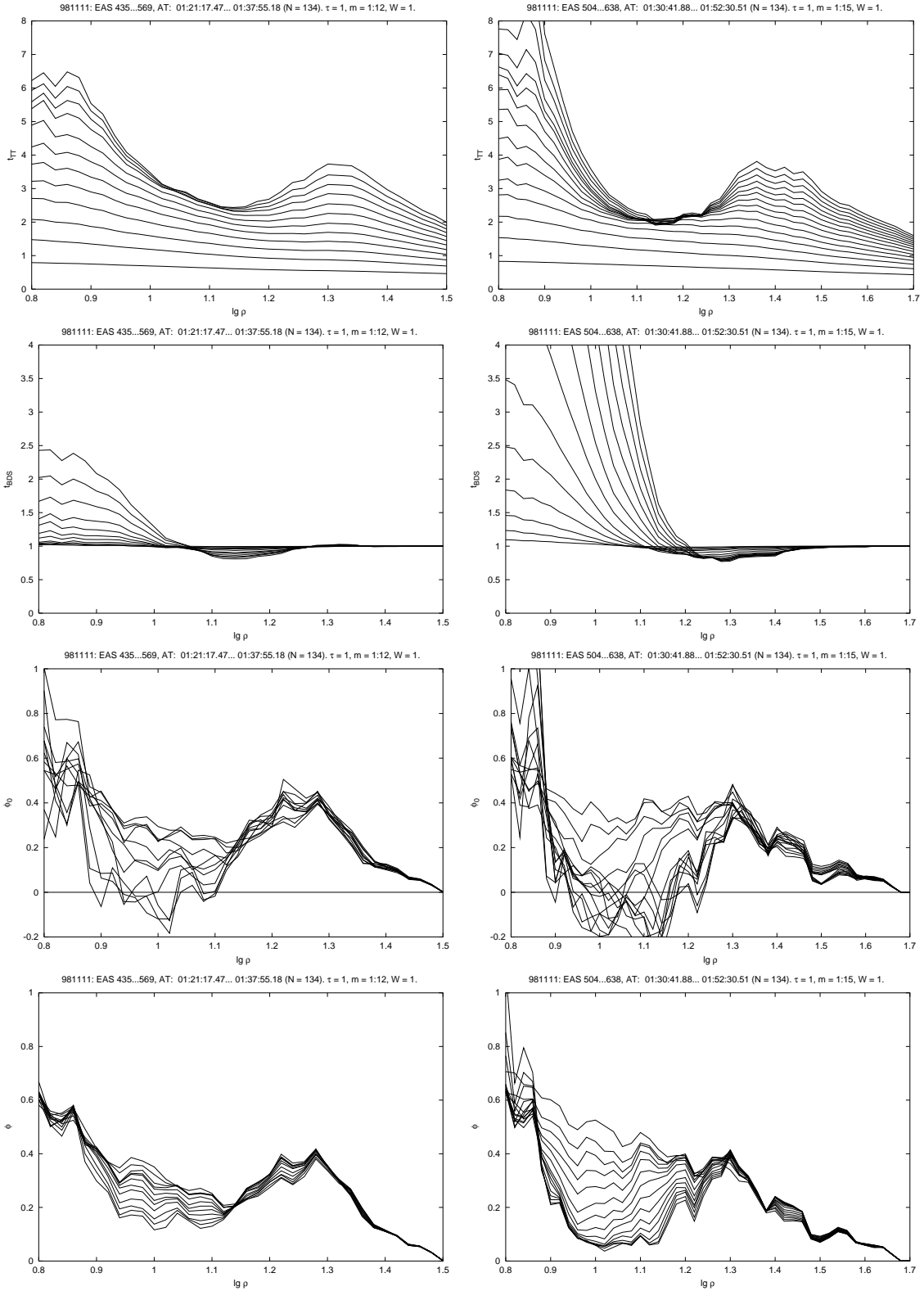


Figure 3: From top to bottom: the Theiler–Takens estimator, see Eq. (2); t_{BDS} , Eq. (3); the function φ_0 given by Eq. (4); the normalized slope φ , Eq. (5). The left column represents the cluster (EAS #435–569), the right column represents EAS #504–638.

and contains, say, the first half of the cluster, it does not have a clear plateau in the $D_2(\rho)$ plot. A plateau appears when the cluster occupies the biggest part of a sample. If we shift a sample further to the end of the cluster, a plateau is observed well, but its level lowers from $D_2 \approx 1.8$ to $D_2 \approx 0.6 \dots 0.8$. It is interesting that a plateau is observed even if a sample has less than a half of the cluster. Thus we conclude that the second half of the cluster influences the dynamics of the correlation dimension more significantly than the first one.

A plateau in the $D_2(\rho)$ plot can also be observed if we increase the length of a sample containing the cluster up to $N \approx 500$. The plateau is more pronounced if a sample contains more of the after-cluster showers than those arrived before. It is interesting that the level of the plateau becomes higher as N grows.

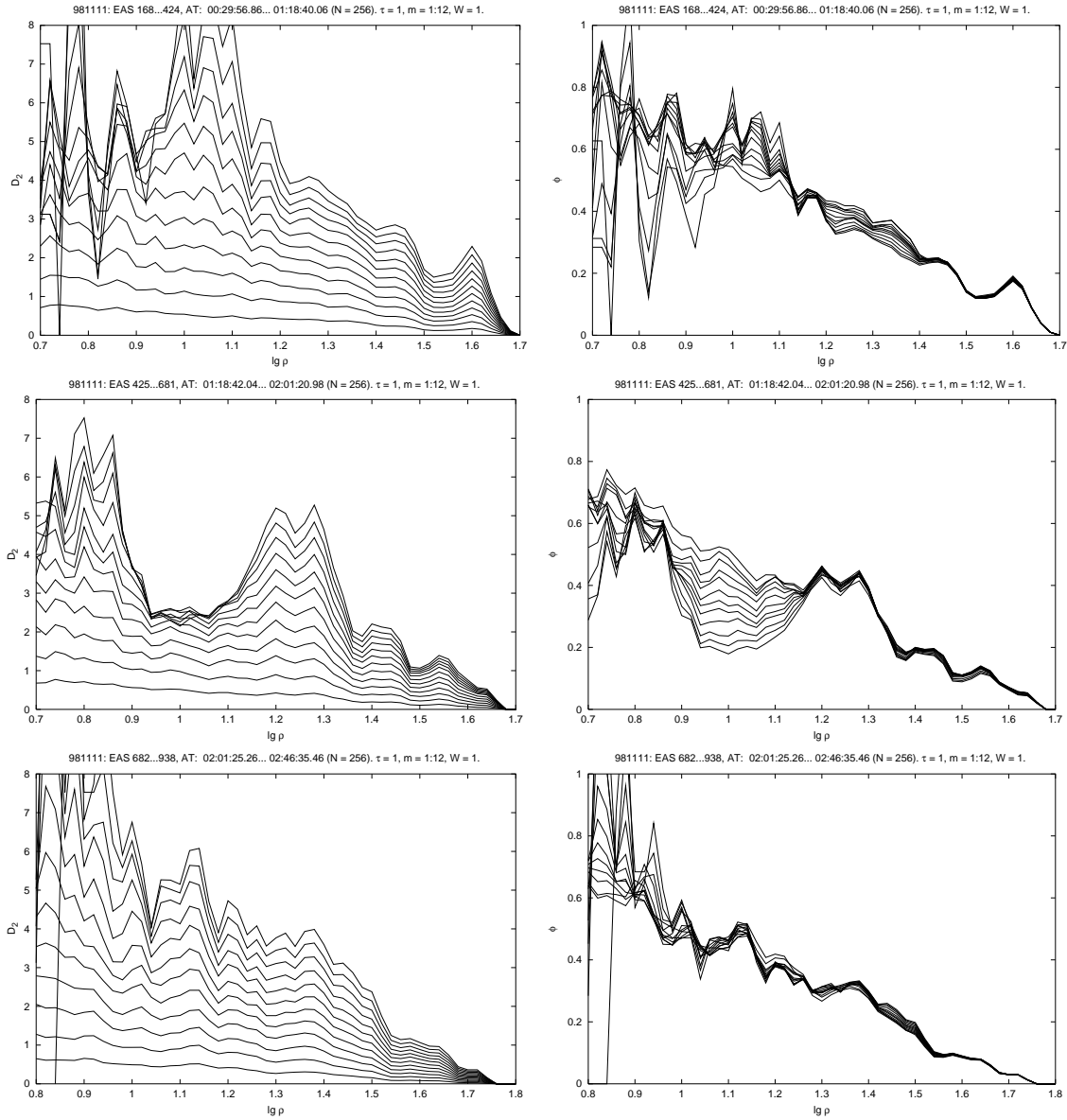


Figure 5: The correlation dimension (the left column) and the normalized slope (the right column) for three consequent samples with $N = 256$. The samples are made up of EAS #168–424, 425–681, and 682–938 (the top, middle, and bottom rows respectively).

As an example, let us consider three samples with $N = 256$. The first sample consists of EAS #168–424. It ends up in less than three minutes before the cluster. The second sample consists of EAS #425–681. It

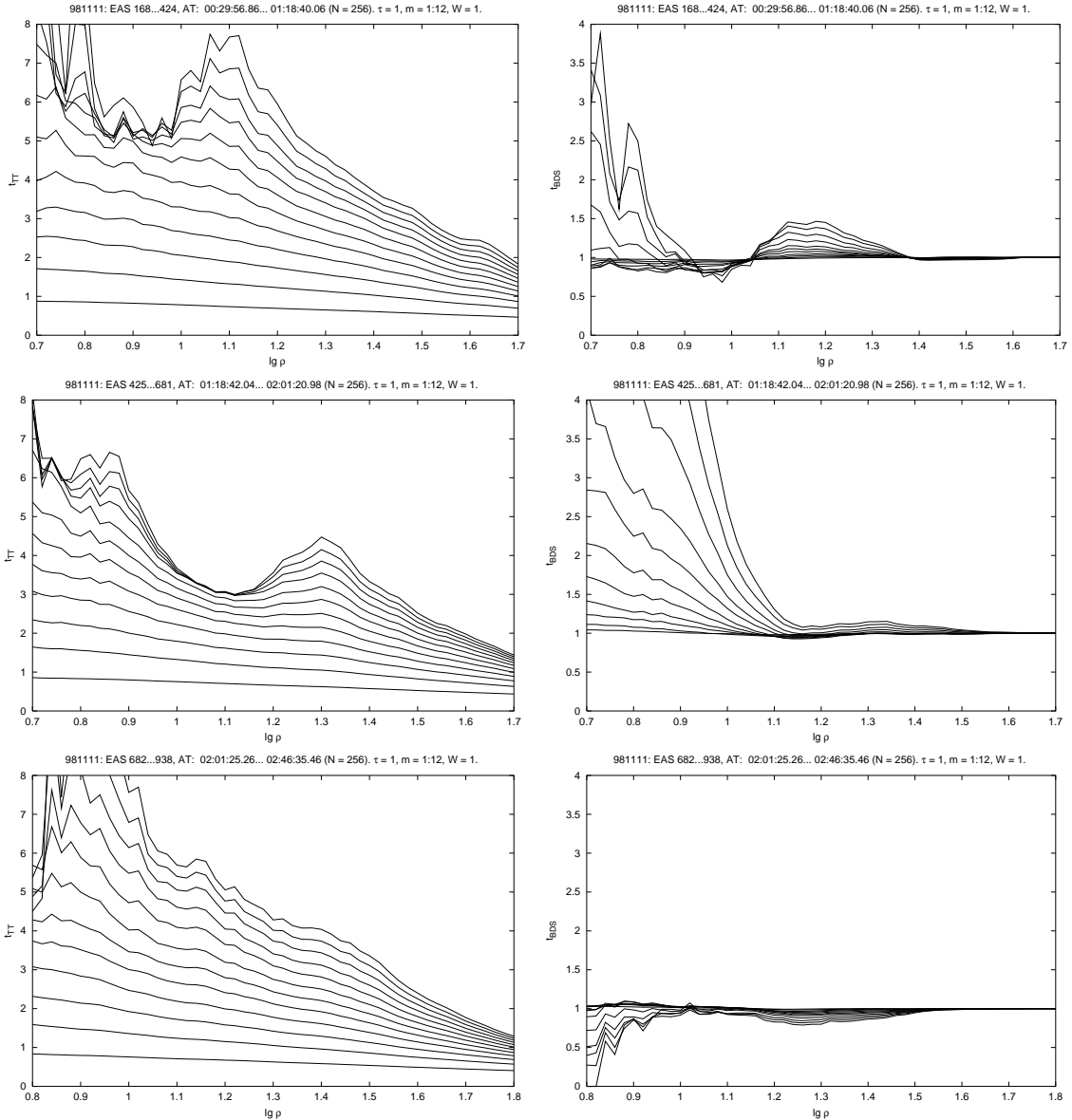


Figure 6: The Theiler–Takens estimator (the left column) and t_{BDS} (the right column) for the same samples as in Fig. 5.

contains the cluster but ends in nearly 23.5 min after the cluster. The last sample consists of EAS #682–938. The choice of these samples is also more or less arbitrary: the correlation dimension does not change qualitatively if we move the boundaries of the samples to the left or to the right in 20 showers or so. Fig. 5 shows the behaviour of the correlation dimension (the left column) and the normalized slope (the right column) for these three samples (from top to bottom). As is clearly seen, the behaviour of D_2 and φ at the interval $\lg \rho \approx 0.94 \dots 1.1$ for the sample that contains the cluster differs qualitatively from that for the samples around the cluster. Namely, D_2 has a plateau with $D_2 \approx 2.5$, and φ has a hollow, at which φ goes down approximately to 0.2 and even down to 0.15 if $m = 15$ is used. (We recall that φ converges slowly, see [13].) Notice that though this value of φ suggests that the sample with the cluster should be treated by statistical rather than by deterministic methods, the behaviour of φ for the samples without a plateau is strikingly different.

Fig. 6 presents the Theiler–Takens estimator t_{TT} and the function t_{BDS} for the same three samples. Evidently, the behaviour of these quantities for the sample that contains the cluster considerably differs

from the other ones. Namely, for the sample with the cluster, t_{TT} has a nearly flat region where the curves saturate for $m \geq 9$, and t_{BDS} deviates considerably from 1 for $\lg \rho < 1.1$. Surprisingly enough, but one can see a kind of plateau in the t_{TT} plot for the sample before the cluster (see the top left plot). Still, the value of K at the interval where this plateau is observed is not sufficient to make definite conclusions, since $\lg K \lesssim 2$ for $m \geq 9$ in comparison with $\lg K > 2$ even for $m = 12$ at the scaling interval for the sample with the cluster; this is also clear from large fluctuations of D_2 at the corresponding plot.

Thus, we again face a situation when it is difficult to make a definite conclusion on the nature of a plateau in the $D_2(\rho)$ plot for a sample that contains the cluster, though it seems more likely to be deterministic. Similar to the sample with EAS #435–569 discussed above, the χ^2 -test applied to the sample with EAS #425–681 makes us reject the hypothesis for an exponential distribution of time delays with at least 90% L.S. For this sample, the measure of time reversibility $\gamma = -0.22$. It is closer to zero than the corresponding values for the other two samples (-0.63 and -0.38 for the sample before and for the sample after the cluster respectively). In all cases, the value of γ lies within the interval of γ -s calculated for 39 surrogates obtained by random shuffling of time delays. (This number of surrogates corresponds to a 95% L.S.)

Besides this, we have found that surrogates constructed for the sample with EAS #425–681 by random shuffling of time intervals x_i do not have a plateau in the $D_2(\rho)$ plot. A similar situation takes place if we use an advanced technique of making surrogate data implemented in the TISEAN package [29]. This technique is based on the amplitude adjusted Fourier transform method proposed in [19]. The TISEAN-made surrogates did not detect time-irreversibility of the original data, too: $\gamma \in (-0.44, 0.45)$ for 39 surrogates. Thus we conclude that while the test for time-reversibility does not detect nonlinearity in these two samples, the behaviour of D_2 gives an argument in favour of chaotic dynamics since the order of time delays x_i occurs to be important in this sample. As is well known, this is typical for a time series generated by a deterministic, but not a stochastic process.

Similar to the above, the sample with the cluster has a high peak at the left end of the spectrum.

Finally, for the samples with $N = 256$, $\tau = 1$ is again the only value of τ that leads to a plateau in the $D_2(\rho)$ plot (we examined $\tau \leq 5$). The dependence on W occurred to be more interesting than for shorter samples. Namely, as W grows, the level of the plateau grows up to $D_2 \approx 3$ reached for $W = 7$. For larger W , the plateau remains at the same level but becomes more narrow (we studied $W \leq 20$).

3.2. January 8, 1999

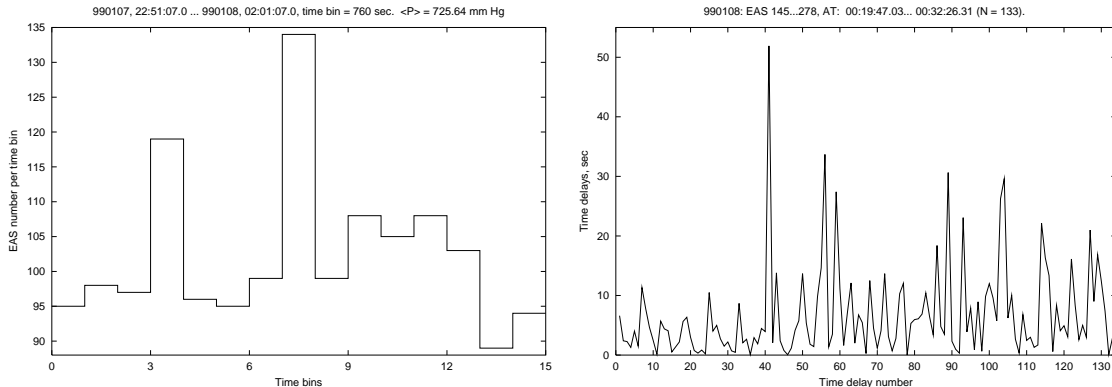


Figure 7: The count rate at a time interval that contains the cluster event registered on January 8, 1999 (left); the outer cluster is presented by the central bin. Time delays (s) between EAS that constitute the outer cluster (right).

An event registered on January 8, 1999 consists of an outer cluster registered between 00:19:47.03 and 00:32:26.31 (Moscow local time) and a number of interior clusters, see Fig. 7 and [4] for the details. The outer cluster consists of 134 EAS (#145–278). It was selected by exactly the same criterion as the cluster registered on November 11, 1998, but demonstrates a drastically different behaviour of the correlation dimension, see Fig. 8 ($\tau = 1$, $m = 1 \dots 15$, $W = 1$). Namely, no plateau is observed. The power spectrum is a broadband

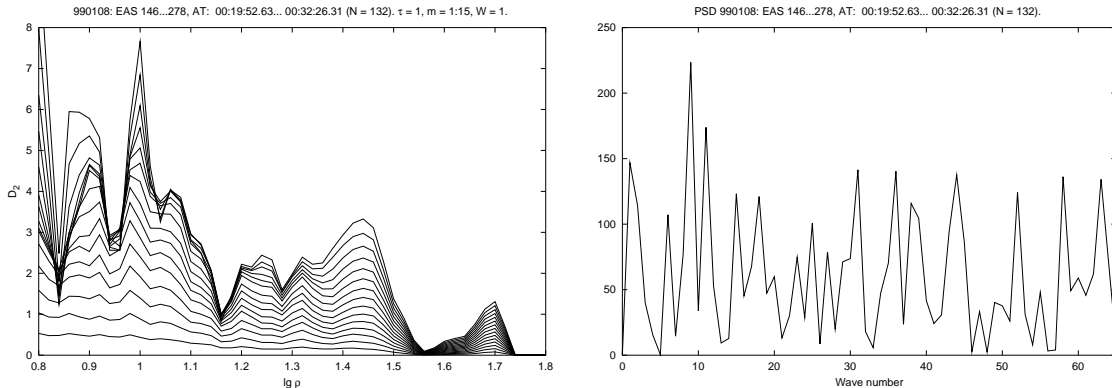


Figure 8: The correlation dimension (left) and the power spectrum density (right) for the outer cluster registered on January 8, 1999 (the first shower is omitted to match the ends of the sample).

one. The measure of time reversibility $\gamma = -0.30$. Besides this, one may accept the hypothesis for an exponential distribution of time delays that form the cluster if 119 delays that do not exceed 14 s are taken into account and 3.5-second time bins are used. Thus, one may conclude that this cluster produces no signs of deterministic chaos in the time series. Still, the situation is not so simple.

If one takes a sample that contains a number of EAS before the cluster and a part of the cluster, then one may observe a sufficiently long plateau in the plot of the correlation dimension, see the second row in Fig. 9. (Here $\tau = 1$ and $W = 1$; for all plots but $D_2(\rho)$, $m = 1 \dots 15$. For the correlation dimension, we use $m = 1 \dots 10$ for clarity.) As one can see, $D_2 \approx 0.9$ at the plateau. Notice that similar to the cluster registered on November 11, 1998 (and especially to the sample consisting of EAS #504–638) the power spectrum density contains a high peak at the beginning of the spectrum, cf. Fig. 4. The sample can be shifted to the left or to the right in approximately twenty EAS without a qualitative difference in D_2 . But the signs of chaotic dynamics in the time series have a short range: the plateau deforms fast if we increase N and disappears for $N \gtrsim 160$. The behaviour of all supplementary functions, i.e., φ , φ_0 , t_{TT} , and t_{BDS} supports the hypothesis that the nature of the plateau in the plot of $D_2(\rho)$ is deterministic, see two bottom rows in Fig. 9.

The surrogate data method also witnesses in favour of this hypothesis in the sense that the plateau is not observed for surrogate data. But again, similar to the situation with the cluster registered on November 11, 1998, the test for time–reversibility does not reject the null hypothesis about linear structure of the underlying process: the original sample has $\gamma = -0.62$ while 39 Fourier-based surrogates give $\gamma \in (-1.43, 1.17)$, and 39 “shuffled” surrogates give $\gamma \in (-1.48, 1.43)$.

Similar to the samples considered above, the result of the χ^2 -test of the hypothesis for an exponential distribution of time intervals that form this sample strongly depends on the choice of time bins. For instance, the hypothesis may be accepted if one takes into account 78 time delays that do not exceed 6 s and uses 1.5-second bins, or if one uses 2.5-second time bins and considers 97 time delays that do not exceed 10 s. In other cases, the hypothesis is rejected with at least 80% L.S.

Similar to the samples discussed above, the behaviour of D_2 does not depend significantly on W . As W grows, the level of the plateau becomes a bit higher reaching $D_2 \approx 1$ for $W \gtrsim 10$. Surprisingly enough, but the value of τ is also not very important for the behaviour of the correlation dimension. Namely, a kind of plateau can be observed for $\tau = 2$ and 3.

Finally, we mention that the use of the maximum norm is important for the appearance of the plateau.

Thus, we have discussed two longest clusters found in our data set. Surprisingly enough, but even much shorter clusters can produce signs of chaotic dynamics in a time series.

3.3. December 28, 1998

The cluster registered on December 28, 1998 consists of 18 EAS having arrived within the time interval from 15:22:33.18 to 15:23:17.34 (Moscow local time) with the atmospheric pressure $P = 740.8$ mm Hg. The showers that form the cluster have numbers 5695–5712 in that day data set. A remarkable feature of this

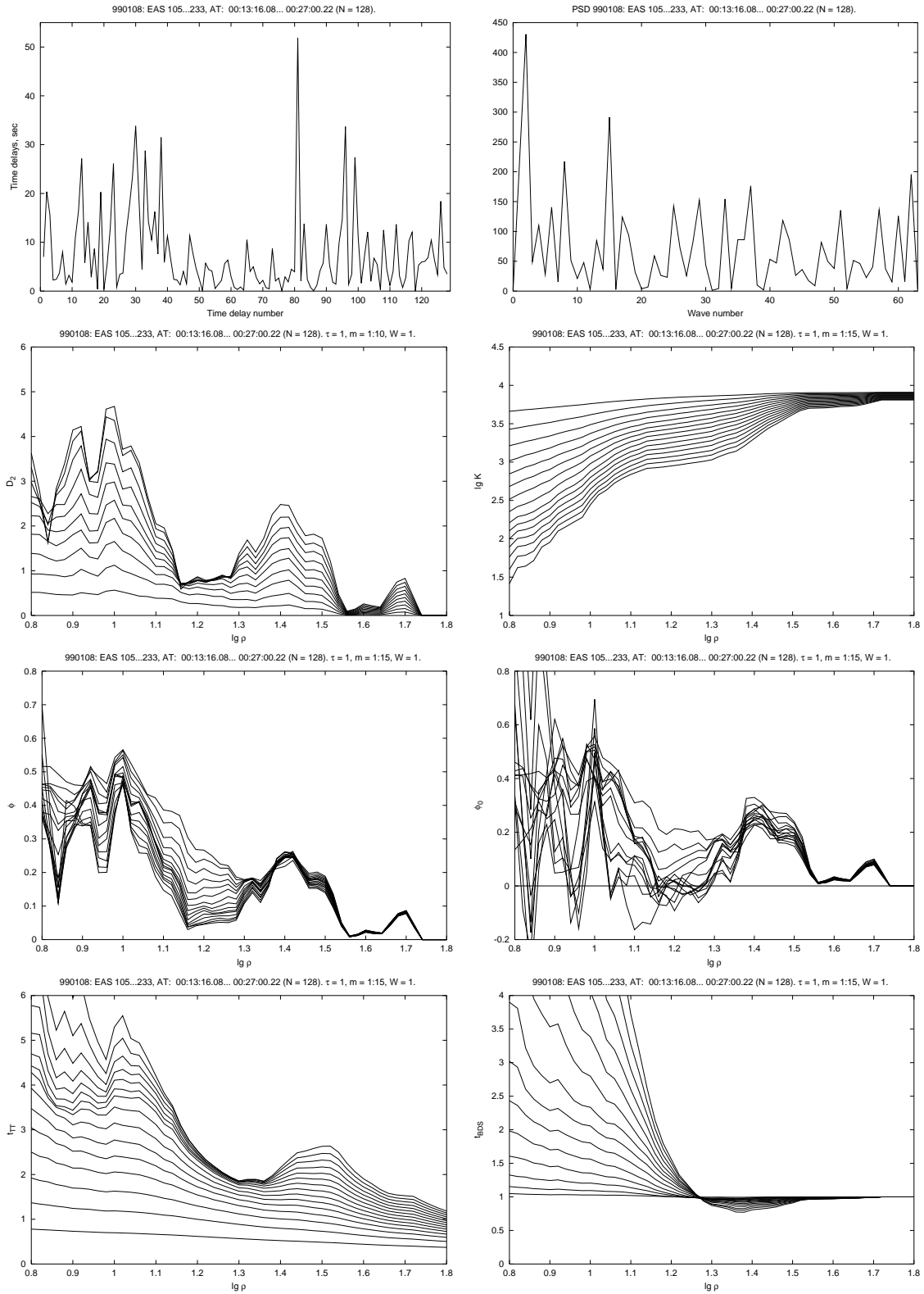


Figure 9: January 8, 1999: A sample that begins 3.5 minutes before the cluster and consists of time delays between EAS #105-232 (the top left plot), its power spectrum density (top right), and miscellaneous quantities: D_2 , $\lg K$, ϕ , ϕ_0 , t_{TR} , and t_{BDS} .

cluster is that its time interval lies within the period of observation of the GRB No. 7285 in the BATSE Catalogs [30].

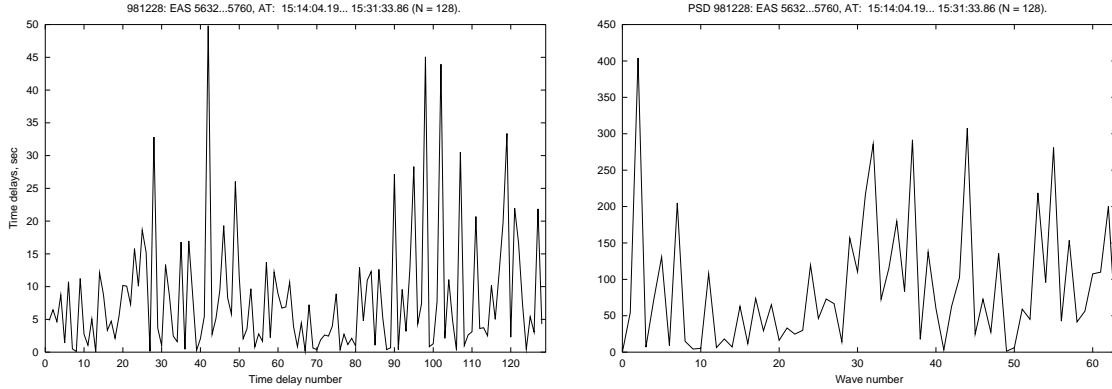


Figure 10: December 28, 1998: time delays (s) for a sample that consists of EAS #5632–5760 (left) and the power spectrum density for this sample (right).

To study this event, we take $N = 128$ and choose a sample that consists of EAS #5632–5760, see Fig. 10. For this sample, $x_1 \approx x_N$. As one can see from the figure, the power spectrum density of the sample has a number of high peaks. Similar to the samples with plateaus discussed above, the highest peak is located at the left end of the spectrum.

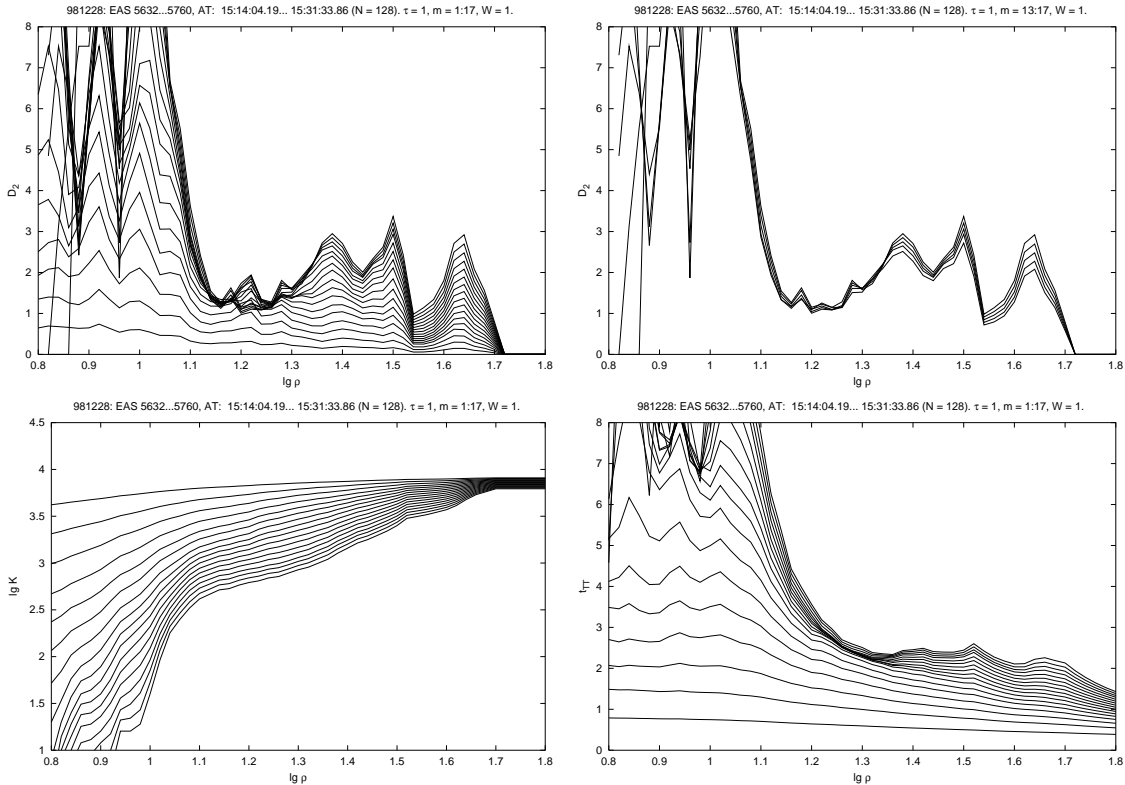


Figure 11: The top row: the correlation dimension D_2 computed for $m = 1 \dots 17$ (left) and $m = 13 \dots 17$ (right). The bottom row: $\lg K$ (left) and the Theiler–Takens estimator t_{TT} (right). For all plots, $\tau = 1$, $W = 1$.

As one can see from Fig. 11, there is an interval $\lg \rho \in (1.14, 1.3)$, at which $D_2(\rho)$ fluctuates around

$D_2 \approx 1.25$. For $m = 5 \dots 11$ these fluctuations are rather high, but become less for $m = 13 \dots 17$. (In fact, these fluctuations can be made smaller if one uses a smoothening procedure to compute D_2 and/or a special choice of the base points.) For this interval, K is large enough, and t_{TT} saturates for $m = 9 \dots 14$. We conclude that the observed behaviour of D_2 and t_{TT} provides signs of chaotic dynamics.

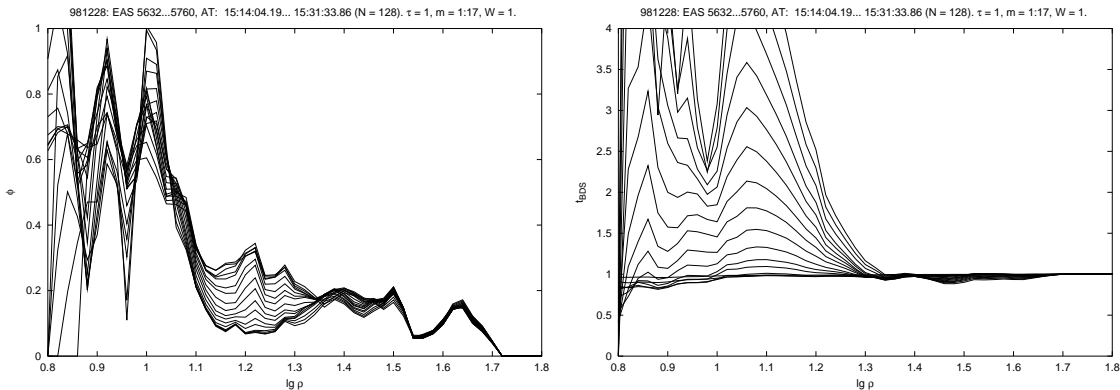


Figure 12: The normalized slope φ (left) and t_{BDS} (right).

Fig. 12 depicts the behaviour of the normalized slope φ and t_{BDS} . It is clearly seen that at the interval of interest, the normalized slope saturates at the value that is less than 0.1, and $t_{BDS} > 1$. The function φ_0 fluctuates around zero at the same interval. All this witnesses in favour of the conjecture that the observed behaviour of the correlation dimension has deterministic nature.

The χ^2 -test of the hypothesis that time intervals that constitute the sample have an exponential distribution revealed that this hypothesis may be accepted if one considers 113 delays that do not exceed 18 s and groups them into 6-second bins, or 119 delays that do not exceed 22.5 s and groups them into 7.5 second bins. For all other ways of grouping time intervals, the hypothesis is rejected with at least 90% L.S. Similar to the above, exponential surrogates do not have a plateau in the $D_2(\rho)$ plot.

The sample shown in Fig. 10 has $\gamma = -0.78$. For 39 shuffled surrogates, $\gamma \in (-1.23, 1.39)$. Consequently, this test reveals that the original time series is likely to have a linear structure. On the other hand, similar to the above, shuffled surrogates do not have a plateau in the $D_2(\rho)$ plot. It is interesting to mention that only two of 39 surrogates have γ that is less than γ computed for the original sample.

The same test performed with the Fourier-based surrogates made with the TISEAN package lead to a surprising result. Namely, for 39 surrogates that preserve both the distribution and the power spectrum density of the original sample, we obtained $\gamma \in (-0.63, 1.40)$. This means that the original sample is *not* time-reversible with a 95% L.S. and thus is nonlinear in the sense of the null hypothesis. We have checked this result with 39 surrogates that preserve only the Fourier power spectrum and obtained the same interval for γ . We stress that this is the only case in our investigation when the surrogate data test witnesses in favour of a nonlinear structure of the experimental time series.

All the quantities discussed earlier in this section were computed for $\tau = 1$ and $W = 1$. We have found that the value of W is not important for the plateau (at least, for $W \leq 20$). For $\tau = 1$, the plateau is clearly observed for $W > 1$, but its level becomes a bit higher, reaching $D_2 \approx 1.5$ for $W \geq 9$. To the contrary, no plateau is observed for $\tau > 1$.

For $N = 128$, the plateau begins to form at samples that contain the cluster at the very end. For instance, its “birth” can be observed at the sample that consists of EAS #5600–5728 and begins at 15:06:56.28. The plateau becomes clearly observed beginning with EAS approximately #5625 registered at 15:12:17.80 and is still observed until the sample that begins at EAS #5640 registered at 15:14:41.16. After this, the plateau begins to deform and disappears approximately at the sample made of EAS #5665–5793 that begins at 15:18:04.49.

If we consider samples that begin at EAS #5632, then the plateau can be observed up to $N \approx 200$ with its level at $D_2 \approx 2$. For larger N , the plateau becomes narrow and then disappears. Thus, the observed behaviour of the correlation dimension has a short time range.

If one uses other norms to compute mutual distances between delay vectors, then a short plateau can be found with for the L_2 and L_{2C} norms with $D_2 \approx 2.2$. Plots of the correlation dimension computed with the L_1 and L_{1C} norms do not have a plateau.

3.4. May 14, 1998

The last event for which we have found a clear plateau in the correlation dimension plot is the cluster registered on May 14, 1998. The fact that this cluster produces signs of chaotic behaviour in the corresponding time series is really remarkable because it is the shortest of the clusters presented in [4]. It consists of only 8 EAS arrived in 4.61 s between 22:24:50.09 and 22:24:54.70 (Moscow local time). The probability of such an event is of the order of $2 \cdot 10^{-8}$. The showers that make the cluster have numbers 7567–7574 in this day data set.

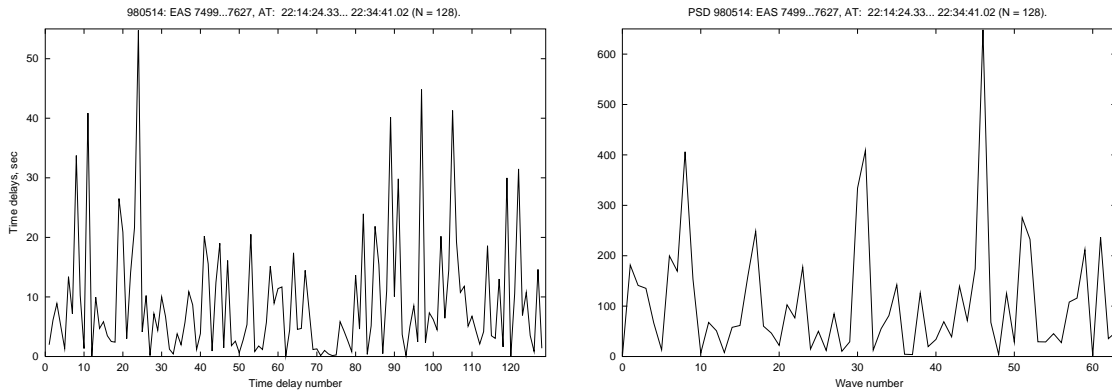


Figure 13: May 14, 1998: time delays (s) for a sample that consists of delays between EAS #7499–7627 (left) and the power spectrum density for this sample (right).

To demonstrate the effect of this cluster on the correlation dimension, we have chosen a sample that consists of 128 time delays between EAS #7499–7627, see Fig. 13. The choice is again more or less arbitrary: we did our best to match the ends of the sample: $x_1 \approx x_N$. As one can see from the figure, the Fourier power spectrum density has three high peaks, but to the contrary to the samples discussed above, none of them is located at the left end of the spectrum.

As one can see from Fig. 14, the correlation dimension has a clear plateau for $\lg \rho \in (1.32, 1.44)$ with $D_2 \approx 1.4$. The number of close delay vectors at this interval exceeds 10^3 . As for the Theiler–Takens estimator, the curves saturate at $\lg \rho \in (1.45, 1.6)$ but not as much as we have seen above. Still, a more or less flat region is observed.

The behaviour of the normalized slope φ and the function φ_0 witness in favour of the conjecture that the plateau in the $D_2(\rho)$ plot has deterministic nature. Namely, as one can see from Fig. 14, at $\lg \rho \in (1.32, 1.44)$, φ tends to a limiting value that is slightly less than 0.1, while φ_0 fluctuates around zero. As for t_{BDS} , it deviates from 1 for $m \geq 10$ and $\lg \rho < 1.44$ but the deviation is comparatively small.

The hypothesis for an exponential distribution of time intervals that make the sample may be accepted if one considers 118 delays that do not exceed 19.5 s and groups them into 8.5-second bins. For all other ways of grouping the intervals, the hypothesis is rejected with at least 90% L.S. Similar to the above, exponential surrogates do not have a plateau in the correlation dimension plots.

For the sample under consideration, the measure of time-reversibility $\gamma = -0.75$. Thirty-nine shuffled surrogates gave $\gamma \in (-1.24, 0.88)$, while 39 Fourier-based surrogates gave $\gamma \in (-1.03, 0.93)$. Thus, the null hypothesis cannot be rejected. Still we mention that only two of 39 Fourier-based surrogates have $\gamma < -0.75$ in comparison with five such surrogates obtained by random shuffling of time delays. None of the surrogates demonstrated a plateau in the $D_2(\rho)$ plot.

Contrary to the above, the plateau occurred to be more sensitive to the value of W for $\tau = 1$. Namely, the plateau is clearly observed for $W \leq 7$. For higher values of W , the plateau becomes distorted and practically disappears for $W > 10$. Simultaneously, t_{BDS} becomes approximately equal to 1.

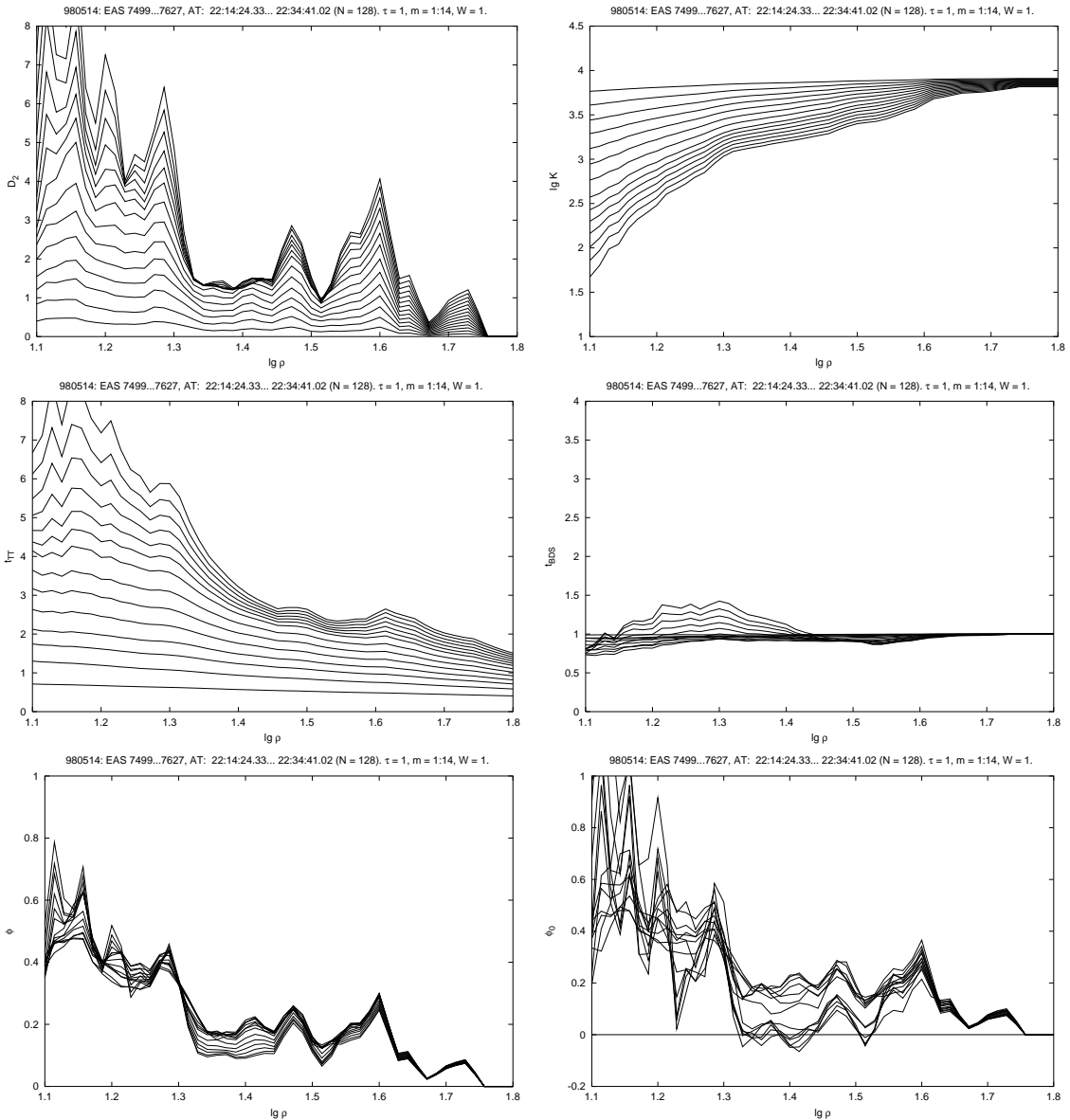


Figure 14: The top row: the correlation dimension D_2 (left) and $\lg K$ (right). The middle row: the Theiler–Takens estimator t_{TT} (left) and t_{BDS} (right). The bottom row: the normalized slope ϕ (left) and ϕ_0 (right).

It is interesting that the plateau is still observed for $\tau = 2$, though it slightly deforms. More precisely, for $\tau = 2$ and $W \geq 1$, the correlation dimension fluctuates around $D_2 \approx 1$ at the interval $\lg \rho \in (1.38, 1.52)$. For $\tau > 2$, the plateau disappears.

For $N = 128$, the plateau is observed for samples that begin at EAS numbers in the range 7490–7530 (this time interval equals 7 min). The plateau is also observed for N up to 190. As N grows, the plateau becomes less wide, and its level increases reaching $D_2 \approx 1.6$ for $N = 190$.

The choice of the maximum norm is crucial for the appearance of the plateau in the $D_2(\rho)$ plot. None of the other used norms produced a clear plateau.

3.5. The Other Cluster Events

None of other sixteen cluster events discussed in [4] produce so clear signs of chaotic dynamics in the time series as the clusters discussed above. Only two of them, namely a cluster found on December 27, 1998 and

a group of embedded clusters registered on January 2, 1999, lead to an appearance of a plateau in the $D_2(\rho)$ plots, but these plateaus are short and not pronounced enough. This may be due to the fact that they lie in the region $\lg \rho \leq 1$ where the number of close delay vectors is not sufficiently large.

4. Discussion

The results presented above demonstrate that one can observe an unusual dynamics of EAS arrival times in the vicinity of certain clusters of EAS with the electron number of the order of 10^5 . Still it is rather difficult to make a final conclusion on the nature of this phenomenon: Does it represent deterministic chaos or a special type of a stochastic process? In our opinion, the majority of the tests performed witness in favour of the first of these two alternatives. Still we must mention that our investigation may somehow suffer of the fact that the phenomena discussed above are only observed at comparatively short time scales with short samples while time series analysis usually prefers longer samples. In connection with this we recall that our investigation of EAS clusters has revealed an existence of “superclusters,” i.e., clusters that have duration more than 30 min and consist of hundreds of EAS. Our future plans include an analysis of these events.

There is a number of other nonlinear tools that may help to make a more definite conclusion about the nature of the observed phenomenon. Among them, one can recall space-time–separation and recurrence plots and a number of other measures of nonlinearity besides the one used above [9]. We also mention that experimental data are inevitably affected by noise that is in particular given by the normal count rate of EAS. To avoid this, signal filtering techniques may be used in future.

On the other hand, as we have already mention above, another big puzzle with signs of chaos in EAS time series is their astrophysical nature. It is likely that clusters that produce signs of chaotic dynamics in the corresponding time series are similar to the upper part of an iceberg in a sense that they do not present the complete process but only the most pronounced part of it. We point out that in all cases considered above the value of the correlation dimension is comparatively small. Since this value gives a (lower) estimate for the dimension of an attractor of the underlying process, it is possible that the structure of this process is not too complicated. Still it seems to be a great challenge to work out a model that could explain chaotic dynamics in EAS arrival times.

It is interesting to compare our results with the conclusions of similar investigations performed by other research groups. In a considerable number of articles devoted to the nonlinear time series analysis, one can find a comprehensive investigation of EAS arrival times registered with the EAS-TOP array [31]. Basing on a detailed study of the available experimental data set and the results obtained with the underground muon monitor [32] the authors of this work made a conclusion that though an existence of deterministic chaotic effects in cosmic ray time series cannot be completely excluded, cosmic ray signals are all color random noise, independently of the nature of the secondary particle and of the primary parent particle. It was also demonstrated in one of the following articles that an impact of background noise brings additional difficulties to the problem of distinguishing between chaotic and stochastic dynamics [33].

Besides this, a whole series of investigations devoted to the nonlinear analysis of EAS time series is carried out in Japan beginning from early nineties at the experimental arrays that now constitute the LAAS network, see, e.g., [34, 35] and references therein. The authors of these investigations presented several dozens of events that demonstrate chaotic dynamics. More than this, it was conjectured that the observed dynamics may be due not only to the chaotic structure of the medium through which particles have traversed but also to the nature of the primary particles [36]. Later on, there was suggested a model according to which chaotic events may be generated by cosmic rays that have a structure of a fractal wave arriving from a nonlinear accelerator like a supernova remnant [37]. This model needs to be studied in details, but seems to be promising.

Thus, the results obtained during our analysis do not contradict the conclusions of similar investigations performed at other EAS arrays. It seems to be necessary to continue the work in this area and to involve some other methods of nonlinear time series analysis.

Acknowledgments

We gratefully acknowledge numerous useful discussions with A. V. Igoshin, A. V. Shirokov, and V. P. Sulakov who have helped us a lot with the experimental data set. We also thank Thomas Schreiber for a very helpful communication. This work was done with financial support of the Federal Scientific-Technical Pro-

gram “Research and design in the most important directions of science and techniques” for 2002–2006, contract No. 40.014.1.1.1110, and by Russian Foundation for Basic Research grant No. 02-02-16081.

Only free, open source software was used for this investigation.

References

- [1] O. V. Vedeneev, N. N. Kalmykov, G. V. Kulikov et al.: “Arrival time distribution of extensive air showers,” *Izv. Ros. Akad. Nauk, Ser. Fiz.* **65** (2001) 1224–1225.
- [2] Yu. A. Fomin, N. N. Kalmykov, G. V. Kulikov et al.: “Distribution of EAS arrival times according to data of the EAS-1000 Prototype array,” Proc. 27th ICRC, Hamburg, 2001, **1**, 195–196; [arXiv: astro-ph/0201343].
- [3] O. V. Vedeneev, M. Yu. Zotov, G. V. Kulikov, Yu. A. Fomin: “EAS clusters with $N_e \sim 5 \times 10^4$,” *Izv. Ros. Akad. Nauk, Ser. Fiz.* **65** (2001) 1674–1677.
- [4] Yu. A. Fomin, G. V. Kulikov, M. Yu. Zotov: “Clusters of EAS with electron number $\gtrsim 10^4$,” Preprint SINP MSU 2002-9/693; [arXiv: astro-ph/0203478].
- [5] M. Yu. Zotov, G. V. Kulikov, Yu. A. Fomin: “Nonlinear analysis of EAS clusters,” *Izv. Ros. Akad. Nauk, Ser. Fiz.* **66** (2002), to appear; [arXiv: astro-ph/0205260].
- [6] N. H. Packard, J. P. Crutchfield, J. D. Farmer, R. S. Shaw: “Geometry from a time series,” *Phys. Rev. Lett.* **45** (1980) 712.
- [7] F. Takens: “Detecting strange attractors in turbulence,” in *Dynamical Systems and Turbulence, Warwick, 1980*, D. A. Rand and L.-S. Young, eds., Lecture Notes in Mathematics, Springer-Verlag, Berlin, 1981, **898** 366–381.
- [8] R. Mañé: “On the dimension of the compact invariant sets of certain non-linear maps,” in *Dynamical Systems and Turbulence, Warwick, 1980*, D. A. Rand and L.-S. Young, eds., Lecture Notes in Mathematics, Springer-Verlag, Berlin, 1981, **898** 230–242.
- [9] T. Schreiber: “Interdisciplinary application of nonlinear time series methods,” *Phys. Rep.* **308** (1999) 1–64; [arXiv: chaos-dyn/9807001].
- [10] P. Grassberger, I. Procaccia: “Characterization of strange attractors,” *Phys. Rev. Lett.* **58** (1983) 2387–2389.
P. Grassberger, I. Procaccia: “Measuring the strangeness of strange attractors,” *Physica D* **9** (1983) 189–208.
- [11] J. Theiler: “Spurious dimension from correlation algorithms applied to limited time series,” *Phys. Rev. A* **34** (1986) 2427.
- [12] M. Frank, H.-R. Blank, J. Heindl et al.: “Improvement of K_2 -entropy calculations by means of dimension scaled distances,” *Physica D* **65** (1993) 359–364.
- [13] A. Potapov, J. Kurths: “Correlation integral as a tool for distinguishing between dynamics and statistics in time series data,” *Physica D* **120** (1998) 369–385.
- [14] F. Takens: “On the numerical determination of the dimension of an attractor,” in *Dynamical Systems and Bifurcations, Groningen, 1984*, B. L. J. Braaksma, H. W. Broer, and F. Takens, eds., Lecture Notes in Mathematics, Springer-Verlag, Berlin, 1985, **1125** 99.
- [15] J. Theiler: “Lacunarity in a best estimator of fractal dimension,” *Phys. Lett. A* **135** (1988) 195.
- [16] A. R. Osborne, A. Provenzale: “Finite correlation dimension for stochastic systems with power-law spectra,” *Physica D* **35** (1989) 357–381.
- [17] A. Provenzale, L. A. Smith, R. Vio, G. Murante: “Distinguishing between low-dimensional dynamics and randomness in measured time series,” *Physica D* **58** (1992) 31–49.
- [18] J. Theiler, D. Prichard: “Constrained-realization Monte-Carlo method for hypothesis testing,” *Physica D* **94** (1996) 221–235.
- [19] J. Theiler, S. Eubank, A. Longtin, B. Galdrikian, J. D. Farmer: “Testing for nonlinearity in time series: the method of surrogate data,” *Physica D* **58** (1992) 77–94.
- [20] T. Schreiber, A. Schmitz: “Improved surrogate data for nonlinearity tests,” *Phys. Rev. Lett.* **77** (1996) 635; [arXiv: chaos-dyn/9909041].
T. Schreiber, A. Schmitz: “Constrained randomization of time series for hypothesis testing,” arXiv: chaos-dyn/9805013.
T. Schreiber: “Constrained randomization of time series data,” *Phys. Rev. Lett.* **80** (1998) 2105; [arXiv:

chao-dyn/9909042].

T. Schreiber, A. Schmitz: “Surrogate time series,” *Physica D* **142** (2000) 346–382; [arXiv: chao-dyn/9909037].

- [21] W. A. Brock, W. D. Dechert, J. A. Scheinkman, B. LeBaron: “A Test for Independence Based on the Correlation Dimension,” University of Wisconsin Press, Madison (1988).
- [22] T. Schreiber, A. Schmitz: “(On the) Discrimination power of measures for nonlinearity in a time series,” *Phys. Rev. E* **55** (1997) 5443; [arXiv: chao-dyn/9909043].
- [23] T. Schreiber: “Determination of the noise level of chaotic time series,” *Phys. Rev. E* **48** (1993) R13–R16.
- [24] A. Schmitz, T. Schreiber: “Testing for nonlinearity in unevenly sampled time series,” *Phys. Rev. E* **59** (1999) 4044; [arXiv: chao-dyn/9804042].
- [25] J.-P. Eckmann, D. Ruelle: “Ergodic theory of chaos and strange attractors,” *Rev. Mod. Phys.* **57** (1985) 617–656.
- [26] Yu. A. Fomin, A. V. Igoshin, N. N. Kalmykov et al.: “New results of the EAS-1000 Prototype operation,” Proc. 26th ICRC, Salt Lake City, 1999, **1** 286–289.
- [27] J. W. Eaton: “GNU Octave: A high-level interactive language for numerical computations,” Edition 3 for version 2.0.13, 1997; <http://www.octave.org/>.
- [28] J. Theiler: “Estimating fractal dimension,” *J. Opt. Soc. Am.* **7** (1990) 1055–1073.
- [29] R. Hegger, H. Kantz, T. Schreiber: “Practical implementation of nonlinear time series methods: The TISEAN package,” *Chaos* **9** (1999) 413; [arXiv: chao-dyn/9810005].
See also <http://www.mpipks-dresden.mpg.de/~tisean>
- [30] The BATSE Gamma Ray Bursts Catalogs, <http://www.batse.msfc.nasa.gov/batse/>
- [31] M. Aglietta, B. Alessandro, F. Arneodo et al.: “Fractal behavior of cosmic ray time series: Chaos or stochasticity?” *J. Geophys. Research* **98** (1993) 15,241–15,254.
- [32] L. Bergamasco, M. Serio, A. R. Osborne: “Correlation dimension of underground muon time series,” *J. Geophys. Research* **97** (1992) 17,153–17,163.
- [33] L. Bergamasco, M. Serio, A. R. Osborne: “The impact of background noise on the determination of the fractal and statistical properties of cosmic ray time series,” *J. Geophys. Research* **99** (1994) 4235–4252.
- [34] T. Kitamura, S. Ohara, T. Konishi et al.: “Chaos in cosmic ray air showers,” *Astropart. Phys.* **6** (1997) 279–291.
- [35] S. Saito, S. Chinomi, T. Harada et al.: “Fractal study of extensive air showers time series,” Proc. 27th ICRC, Hamburg, 2001, **1** 212–215.
- [36] M. Chikawa, N. Hasebe, Y. Katayose et al.: “EASs showing chaotic feature over very long distance,” Proc. 24th ICRC, Rome, 1995, **1** 277–280.
- [37] S. Ohara, T. Konishi, Y. Kato et al.: “Chaos in cosmic rays: A fractal wave model,” Proc. 27th ICRC, Hamburg, 2001, **1** 208–211.

Appendix: Additional Figures

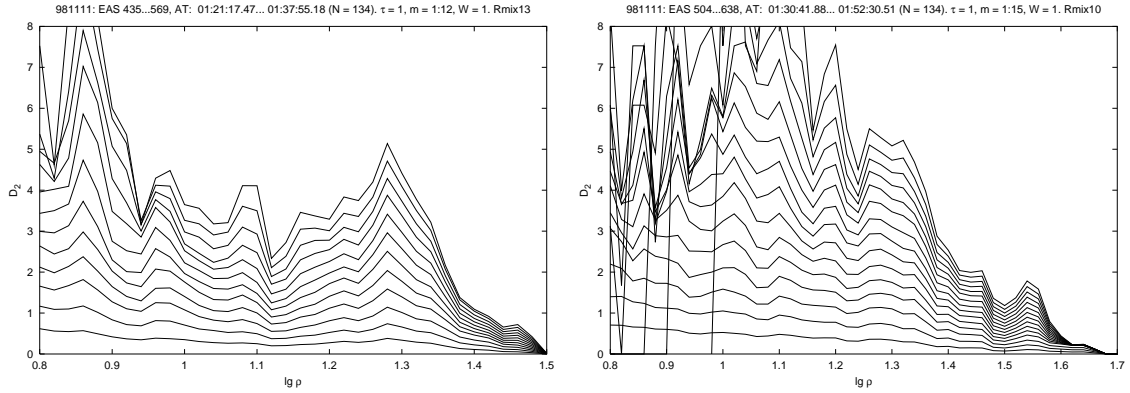


Figure 15: November 11, 1998: The correlation dimension for typical surrogates made by random shuffling of time delays that form the cluster (left) and the sample with EAS #504–638 (right).

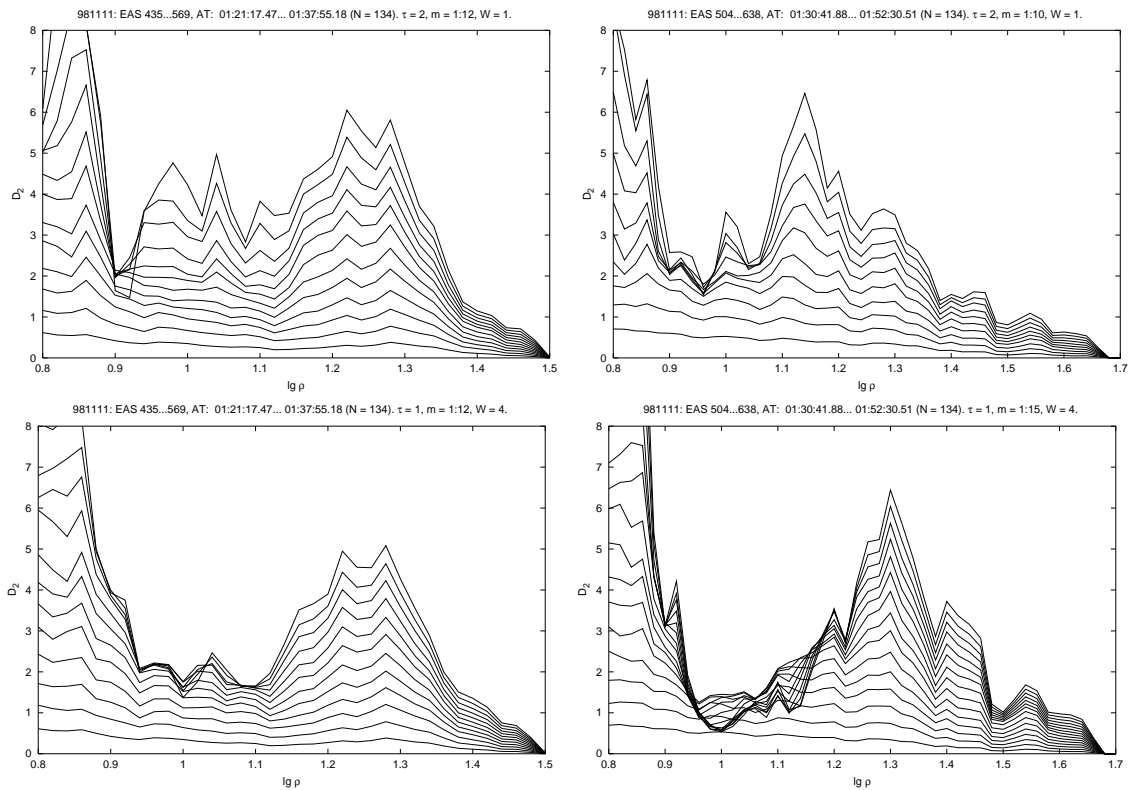


Figure 16: November 11, 1998: The correlation dimension for the samples made of EAS #435–569 (the left column) and EAS #504–638 (the right column) computed for $\tau = 2$, $W = 1$ (the upper row) and $\tau = 1$, $W = 4$ (the bottom row).

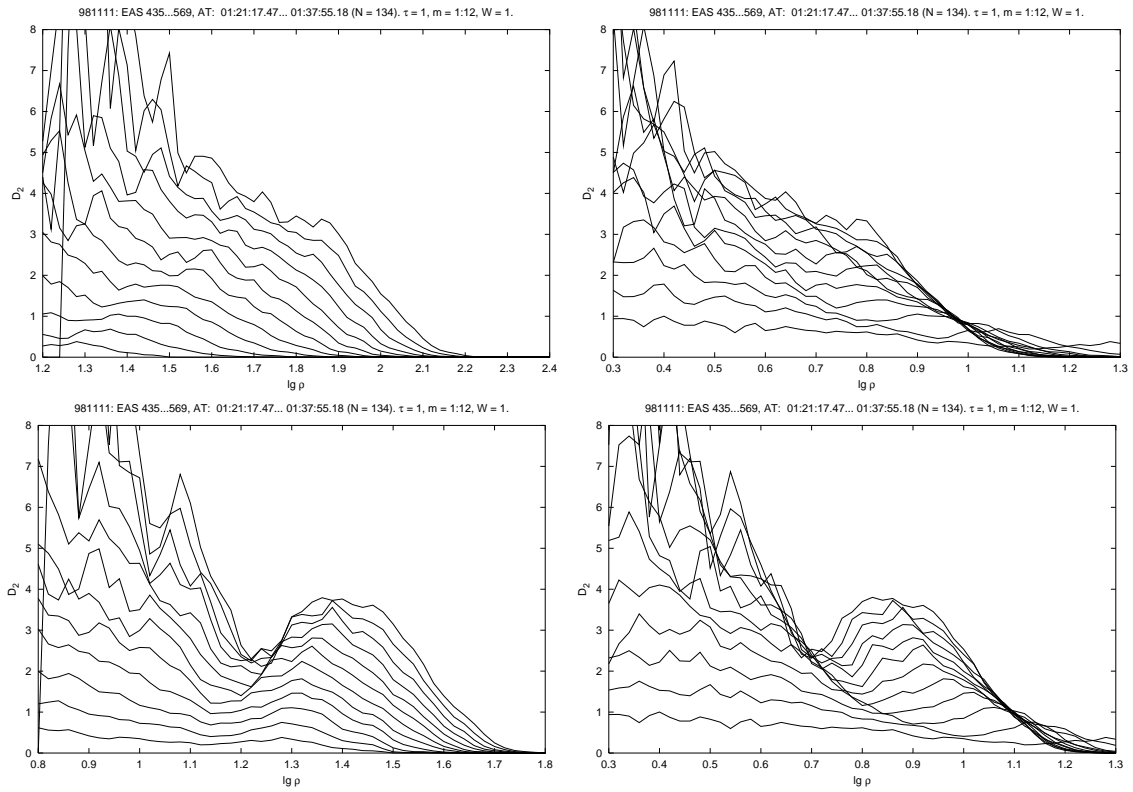


Figure 17: November 11, 1998: The correlation dimension for the sample made of EAS #435–569 computed in different norms: L_1 , L_{1C} (the top row, the left and right plots respectively), L_2 , and L_{2C} (the bottom row).

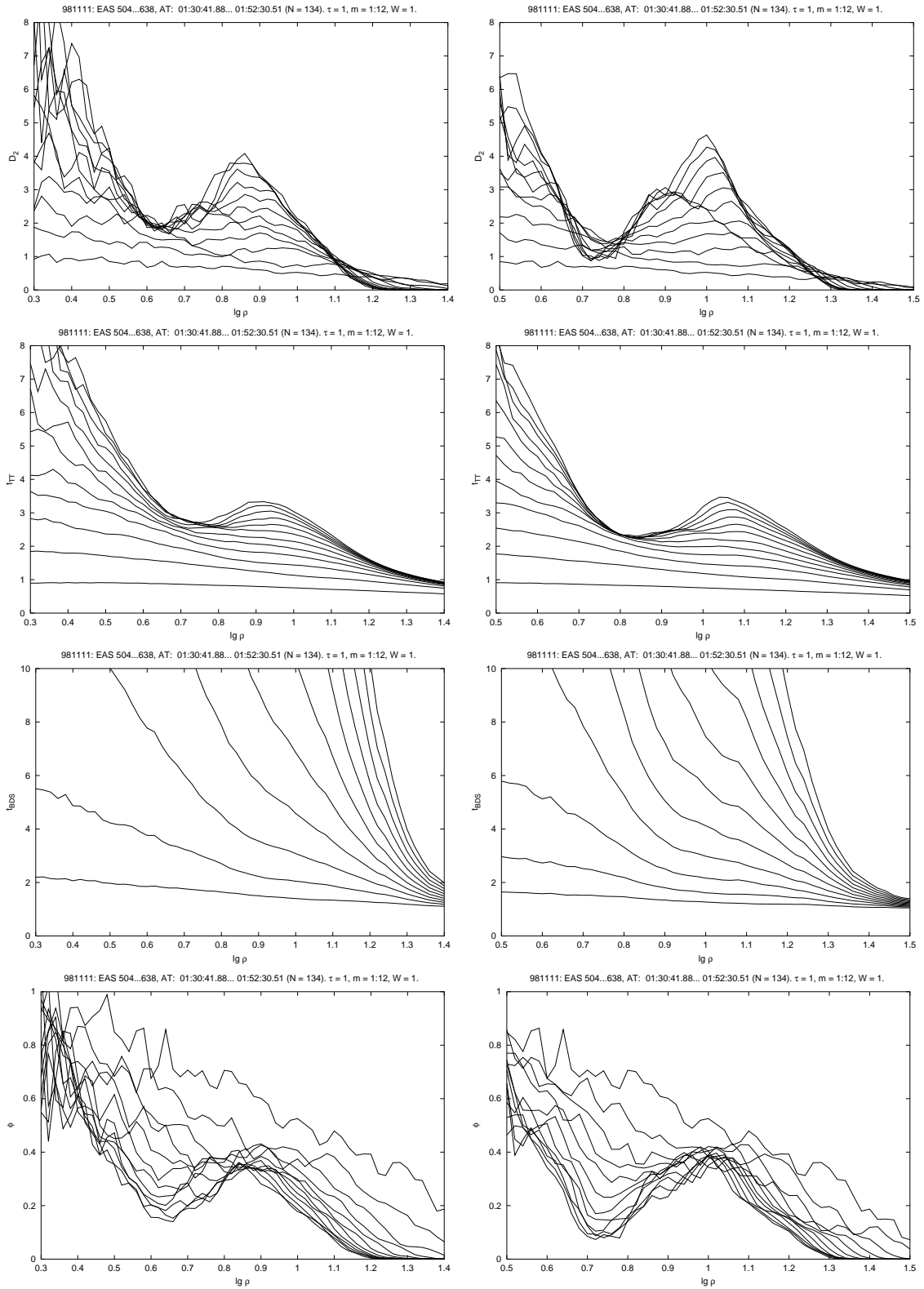


Figure 18: November 11, 1998: Different quantities computed for EAS #504–638 with the norms L_{1C} (the left column) and L_{2C} (the right column). From top: D_2 , t_{TT} , t_{BDS} , and ϕ .

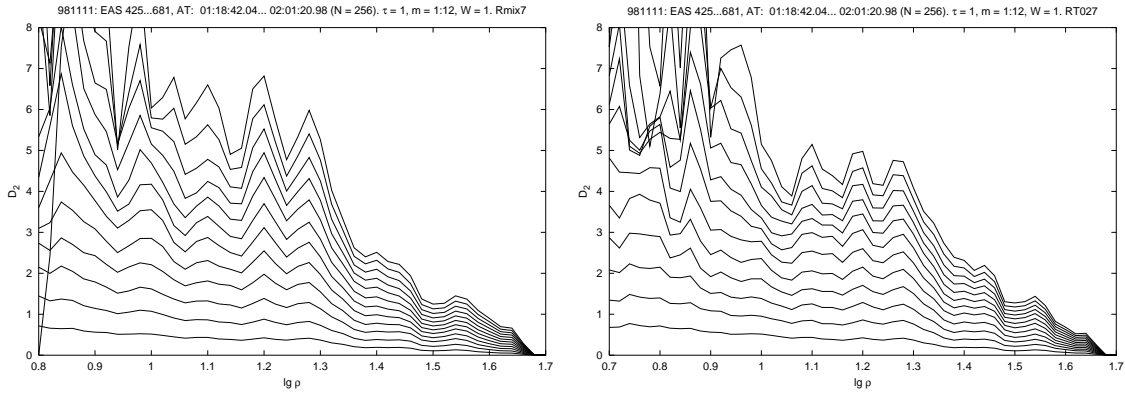


Figure 19: November 11, 1998: Typical behaviour of the correlation dimension for surrogates made for the sample with EAS #425–681 by random shuffling of time delays (left) and by the amplitude adjusted Fourier transform method (right).

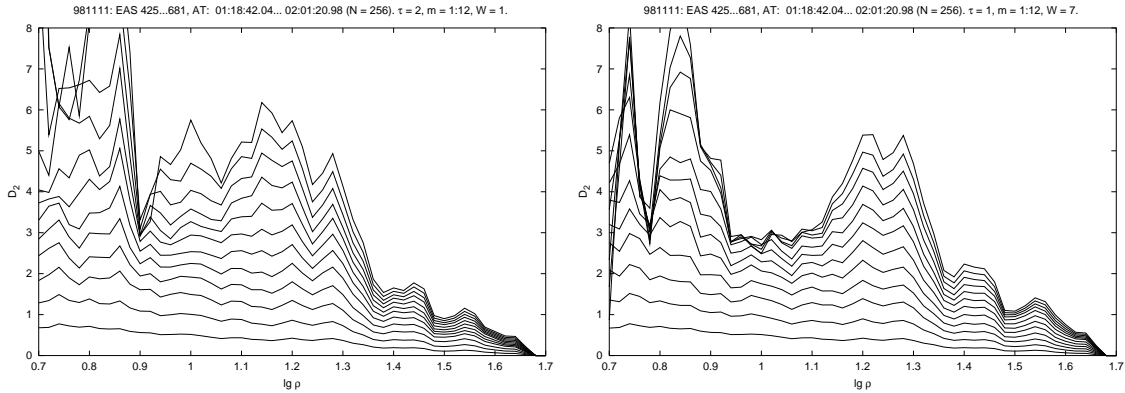


Figure 20: November 11, 1998: The correlation dimension for the sample made of EAS #425–681 calculated for $\tau = 2$, $W = 1$ (left) and $\tau = 1$, $W = 7$ (right).

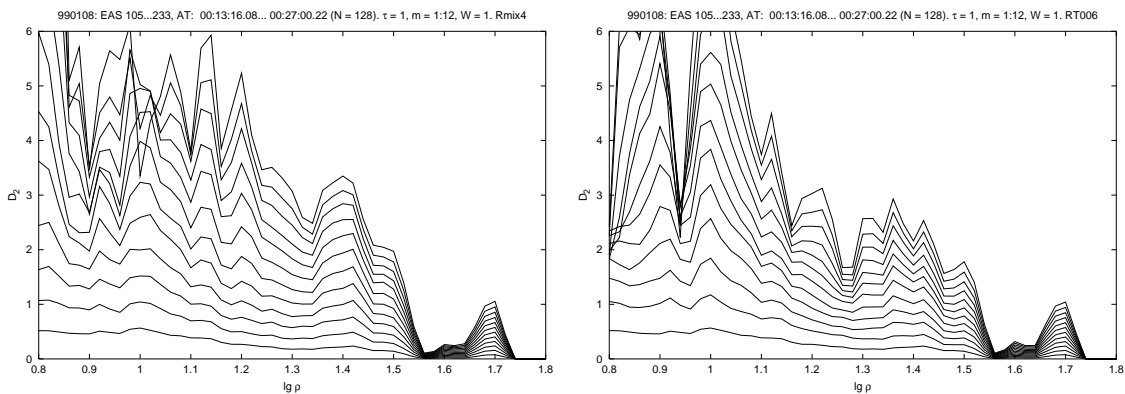


Figure 21: January 8, 1999: Typical behaviour of the correlation dimension for surrogate data created for the sample made of time delays between EAS #105–233. Left: D_2 for randomly shuffled data. Right: D_2 for a Fourier-based surrogate.

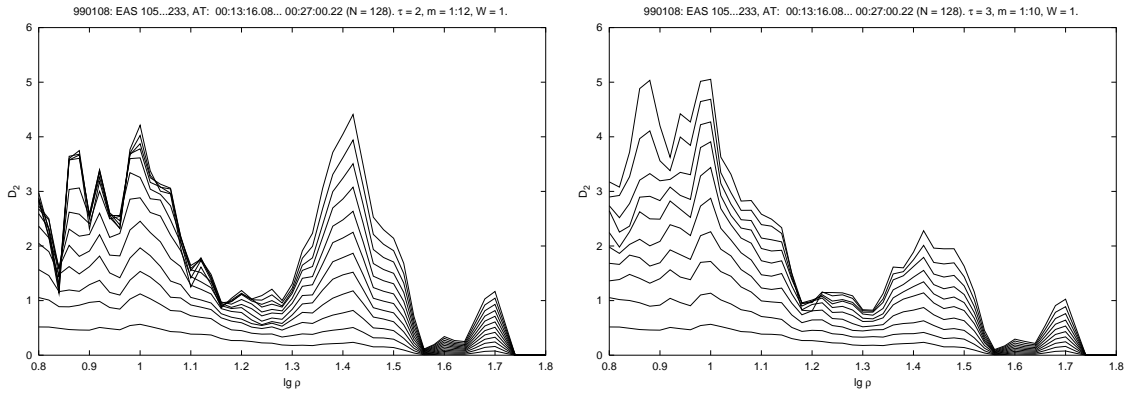


Figure 22: January 8, 1999: The correlation dimension for the sample made of time delays between EAS #105–233 for $\tau = 2$ (left) and $\tau = 3$ (right).

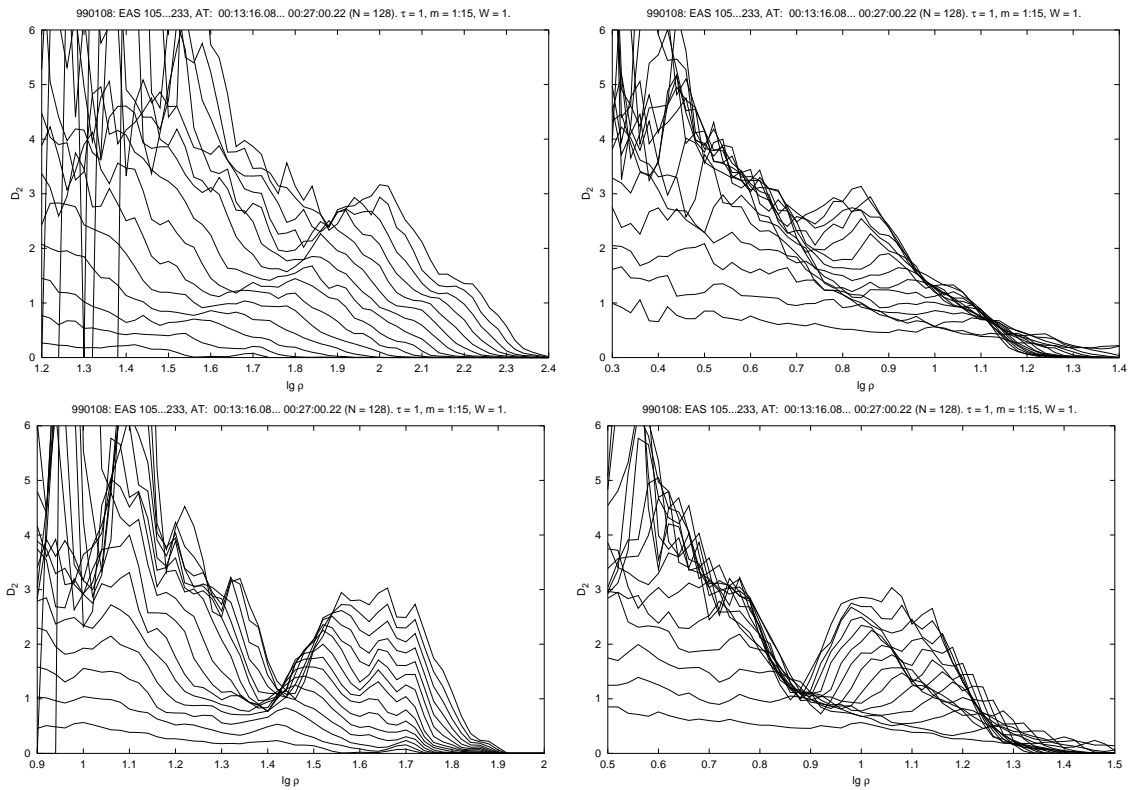


Figure 23: January 8, 1999: The correlation dimension for the sample made of time delays between EAS #105–233 computed in different norms: L_1 , L_{1C} (the top row, the left and right plots respectively), L_2 , and L_{2C} (the bottom row).

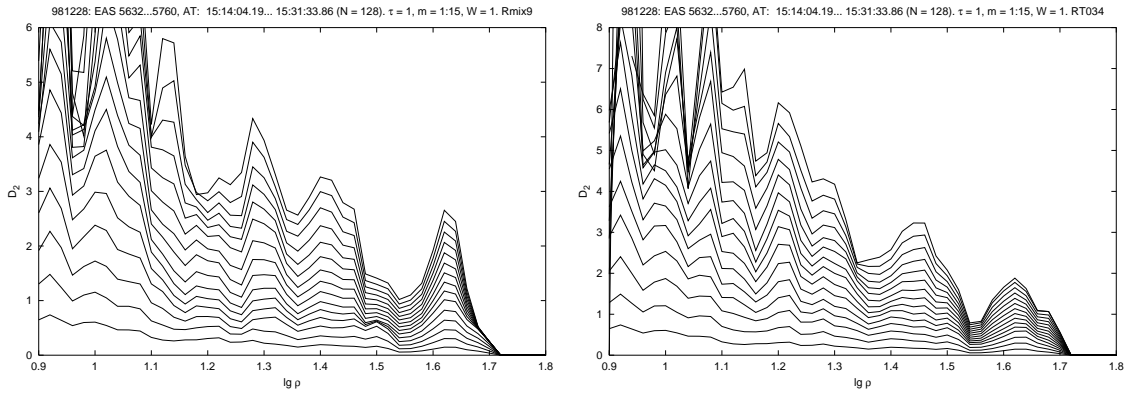


Figure 24: December 28, 1998: Typical behaviour of the correlation dimension for a shuffled and a TISEAN-made surrogate (the left and right plots respectively).

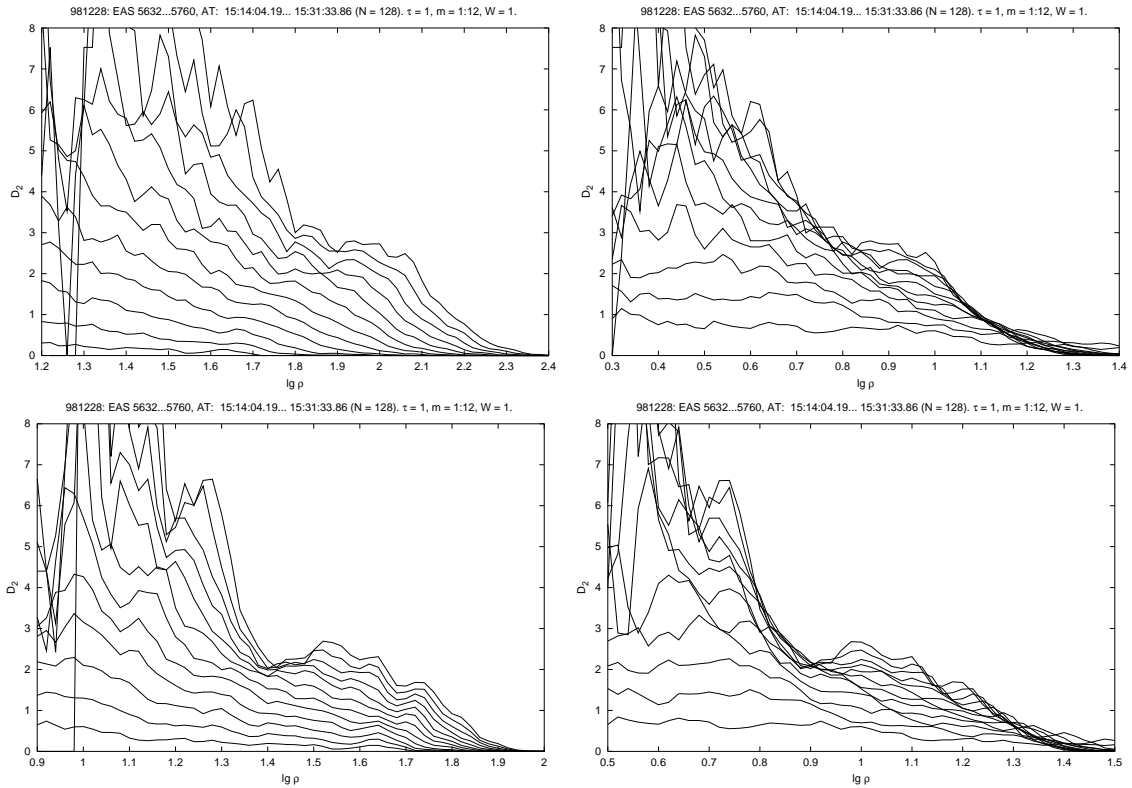


Figure 25: December 28, 1998: The top row: the correlation dimension D_2 computed with the L_1 and L_{1C} norms (the left and right plots respectively). The bottom row: the same but for the norms L_2 and L_{2C} .

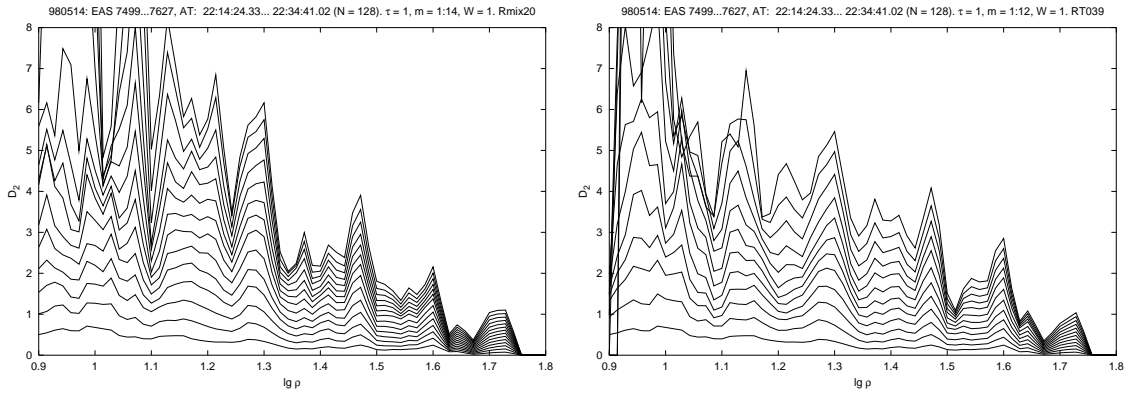


Figure 26: May 14, 1998: Typical behaviour of the correlation dimension for shuffled and TISEAN-made surrogates (the left and right plots respectively).

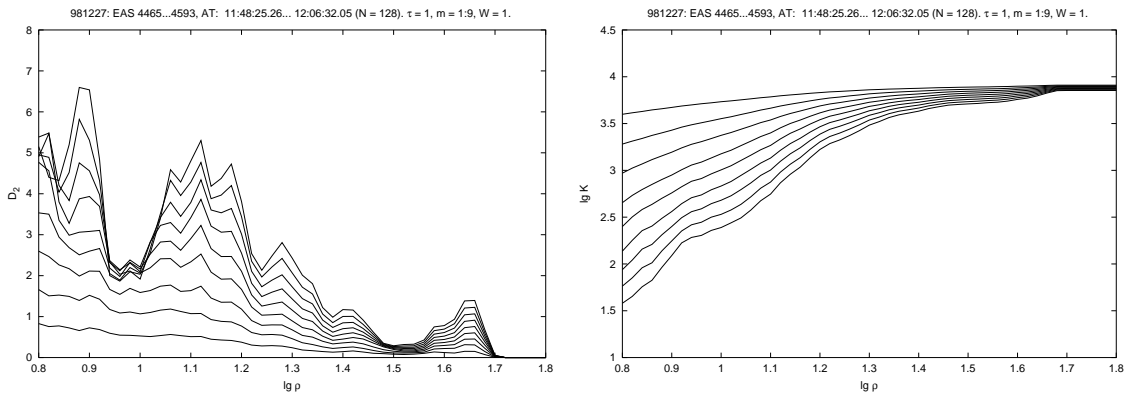


Figure 27: The correlation dimension (left) and the correlation sum (right) for a sample that contains the cluster registered on December 27, 1998.